



US008858816B2

(12) **United States Patent**
Godet et al.

(10) **Patent No.:** **US 8,858,816 B2**
(45) **Date of Patent:** **Oct. 14, 2014**

(54) **ENHANCED ETCH AND DEPOSITION
PROFILE CONTROL USING PLASMA
SHEATH ENGINEERING**

C03C 25/68 (2006.01)
C23F 1/00 (2006.01)
H01J 37/32 (2006.01)
C23C 16/50 (2006.01)
C23C 16/04 (2006.01)

(71) Applicant: **Varian Semiconductor Equipment
Associates, Inc.**, Gloucester, MA (US)

(52) **U.S. Cl.**
CPC *B44C 1/227* (2013.01); *H01J 37/32623*
(2013.01); *H01J 37/32412* (2013.01); *H01J*
2237/3345 (2013.01); *H01J 2237/3344*
(2013.01); *C23C 16/50* (2013.01); *C23C*
16/045 (2013.01)

(72) Inventors: **Ludovic Godet**, Boston, MA (US);
Timothy Miller, Ipswich, MA (US);
George Papasouliotis, North Andover,
MA (US); **Vikram Singh**, Andover, MA
(US)

USPC **216/67**
(58) **Field of Classification Search**
USPC 216/67
See application file for complete search history.

(73) Assignee: **Varian Semiconductor Equipment
Associates, Inc.**, Gloucester, MA (US)

(*) Notice: Subject to any disclaimer, the term of this
patent is extended or adjusted under 35
U.S.C. 154(b) by 0 days.

(56) **References Cited**

U.S. PATENT DOCUMENTS

2008/0179546 A1* 7/2008 Lee et al. 250/492.21
* cited by examiner

(21) Appl. No.: **14/055,121**

Primary Examiner — Roberts Culbert

(22) Filed: **Oct. 16, 2013**

(65) **Prior Publication Data**

US 2014/0034611 A1 Feb. 6, 2014

(57) **ABSTRACT**

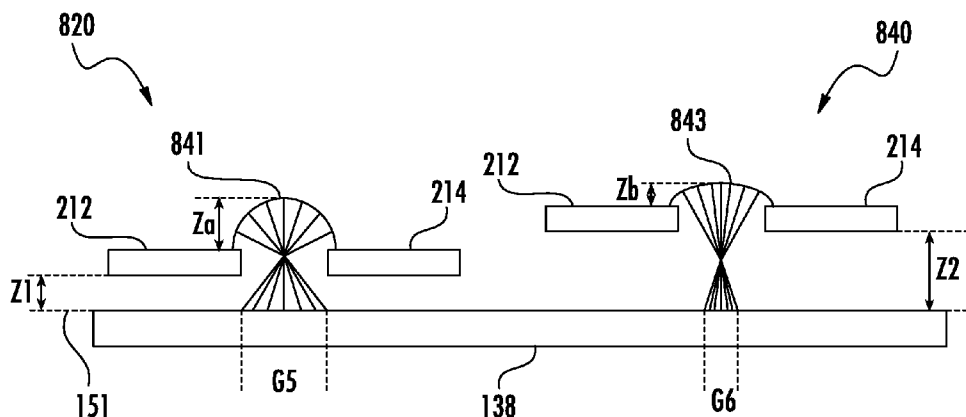
Related U.S. Application Data

(60) Division of application No. 12/645,638, filed on Dec.
23, 2009, now Pat. No. 8,603,591, which is a
continuation-in-part of application No. 12/644,103,
filed on Dec. 22, 2009, now Pat. No. 8,101,510, which
is a continuation-in-part of application No.
12/418,120, filed on Apr. 3, 2009, now Pat. No.
8,623,171.

A plasma processing tool is used to deposit material on a
workpiece. For example, a method for conformal deposition
of material is disclosed. In this embodiment, the plasma
sheath shape is modified to allow material to impact the
workpiece at a range of incident angles. By varying this range
of incident angles over time, a variety of different features
can be deposited onto. In another embodiment, a plasma processing
tool is used to etch a workpiece. In this embodiment, the
plasma sheath shape is altered to allow ions to impact the
workpiece at a range of incident angles. By varying this range
of incident angles over time, a variety of differently shaped
features can be created.

(51) **Int. Cl.**
B44C 1/22 (2006.01)
C03C 15/00 (2006.01)

9 Claims, 22 Drawing Sheets



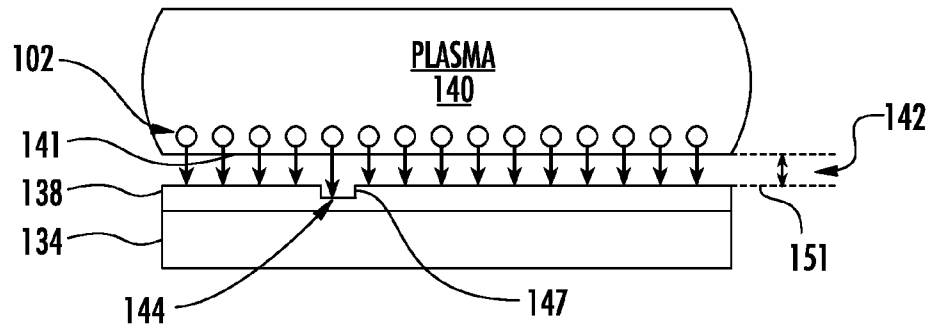


FIG. 1
PRIOR ART

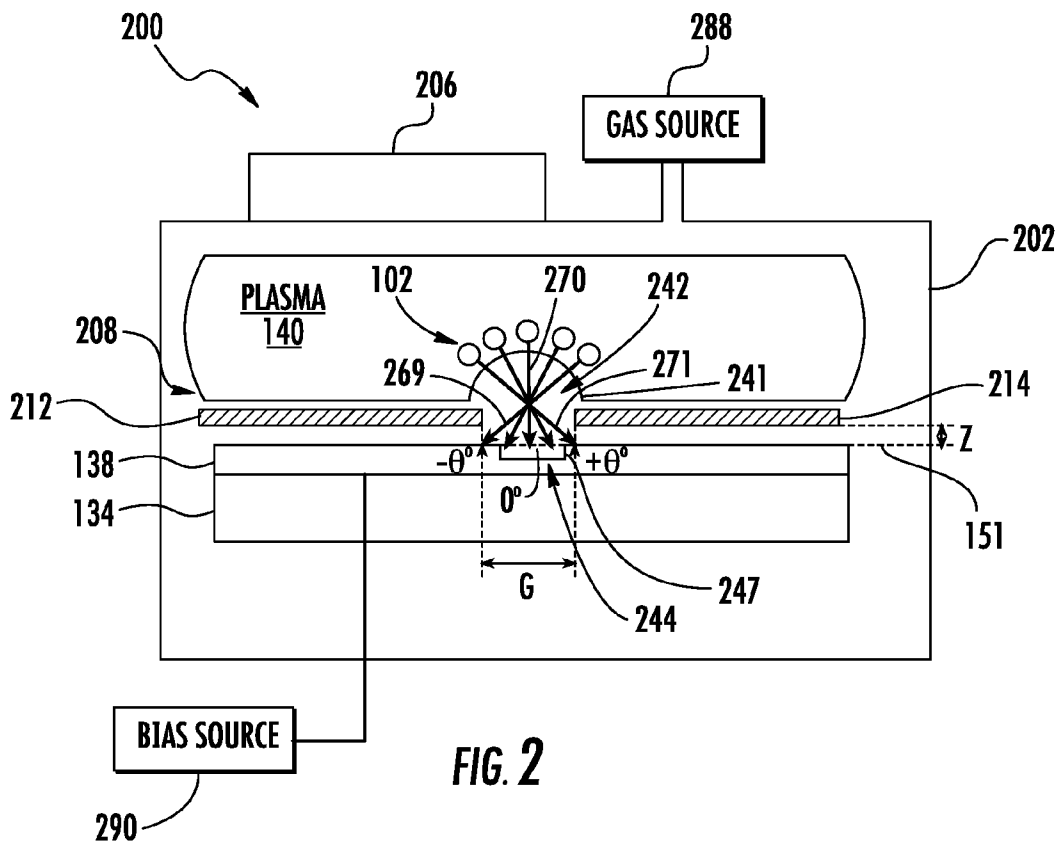


FIG. 2

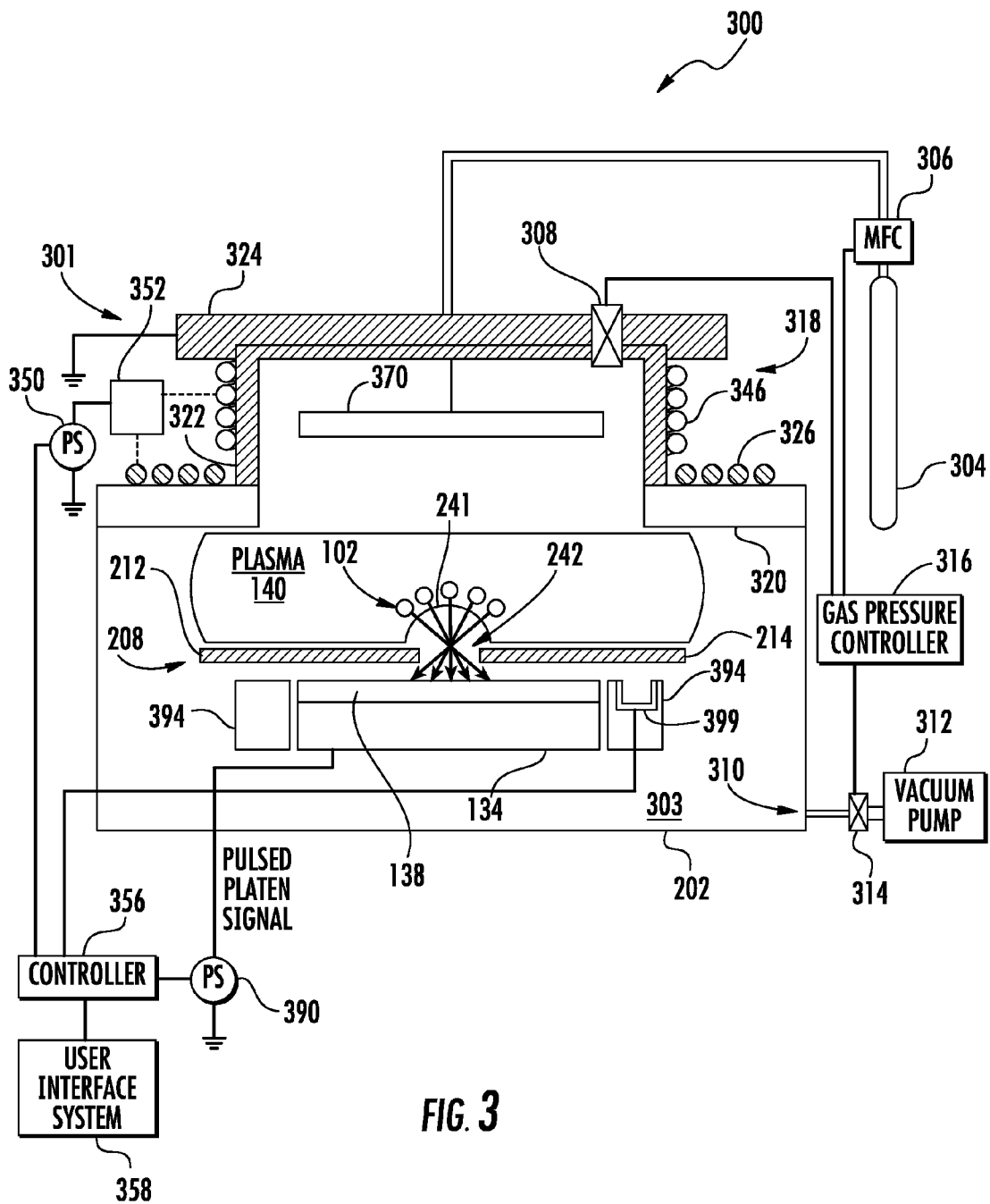
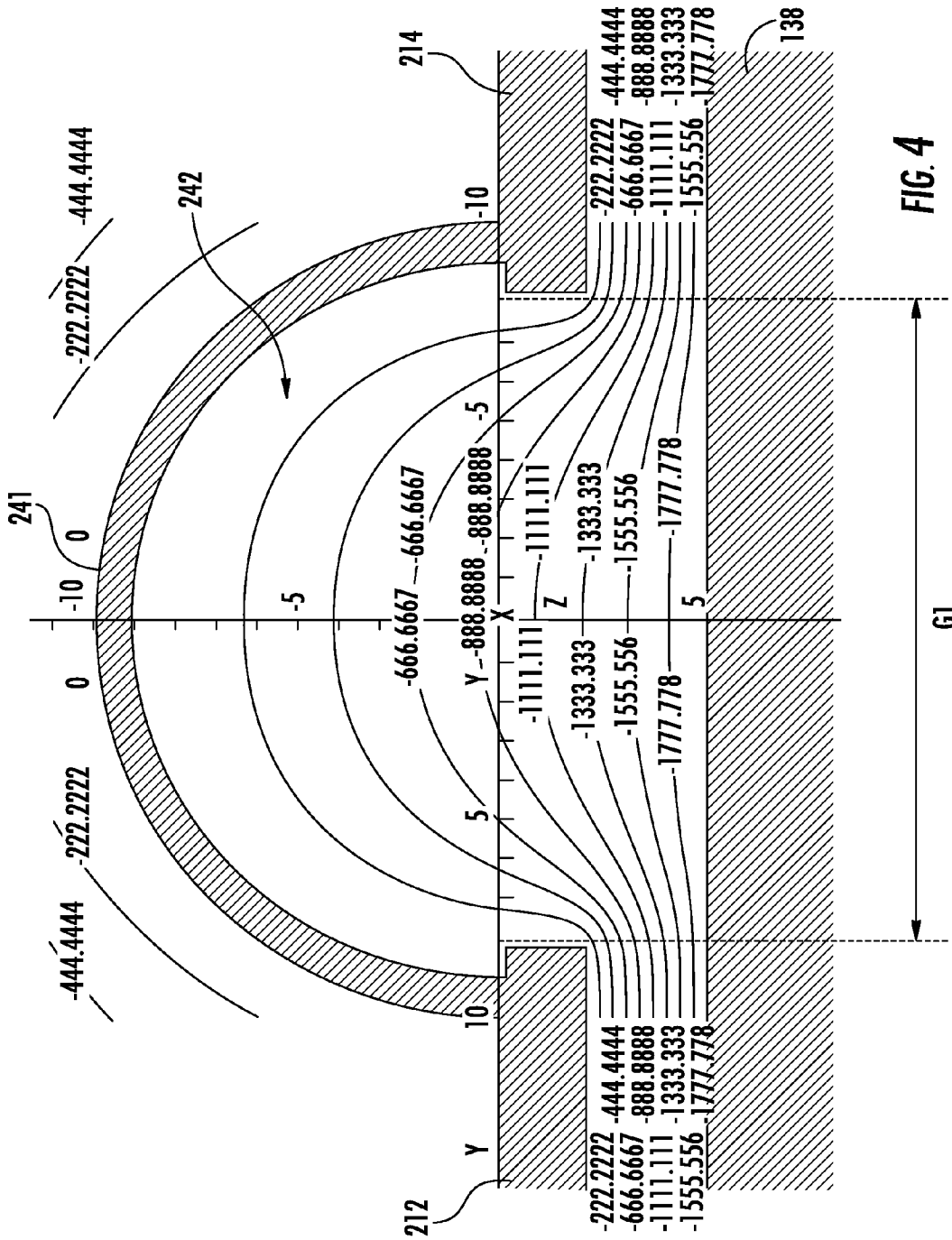


FIG. 3



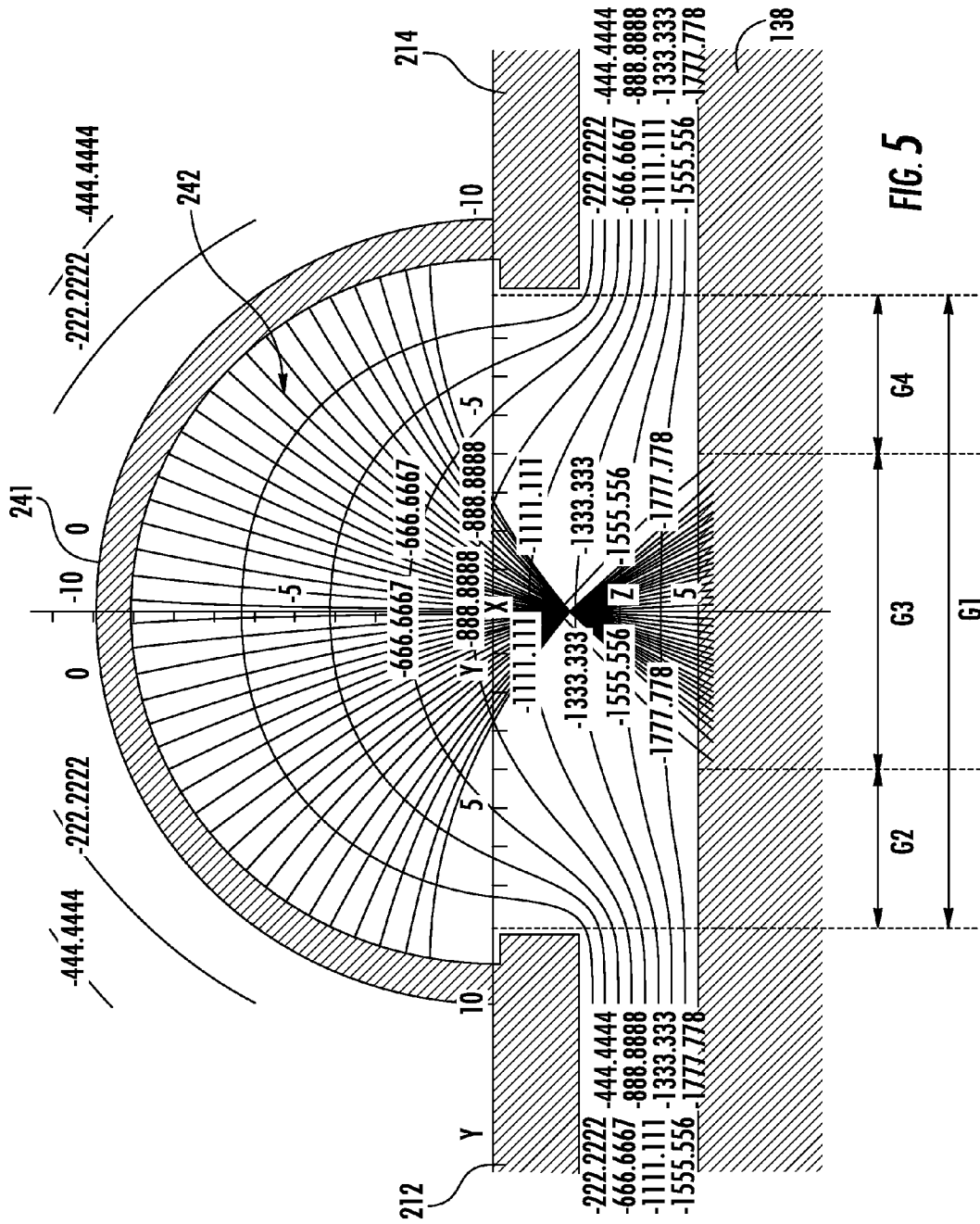


FIG. 5

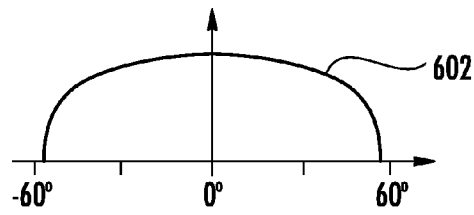


FIG. 6

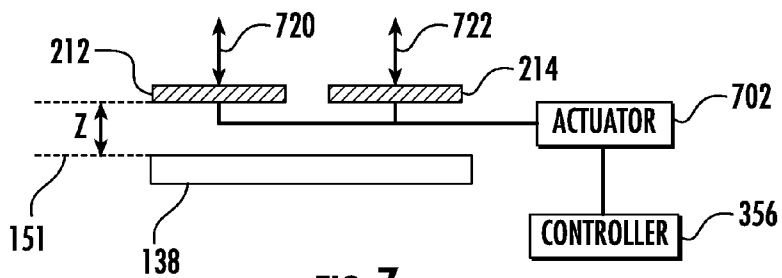


FIG. 7

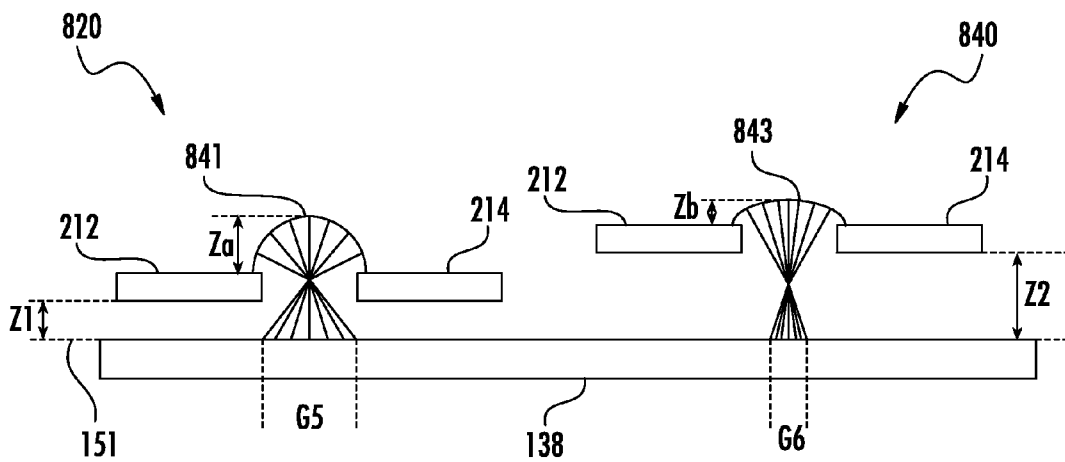


FIG. 8

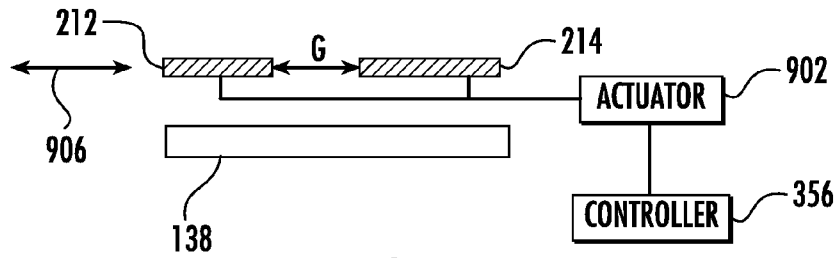


FIG. 9

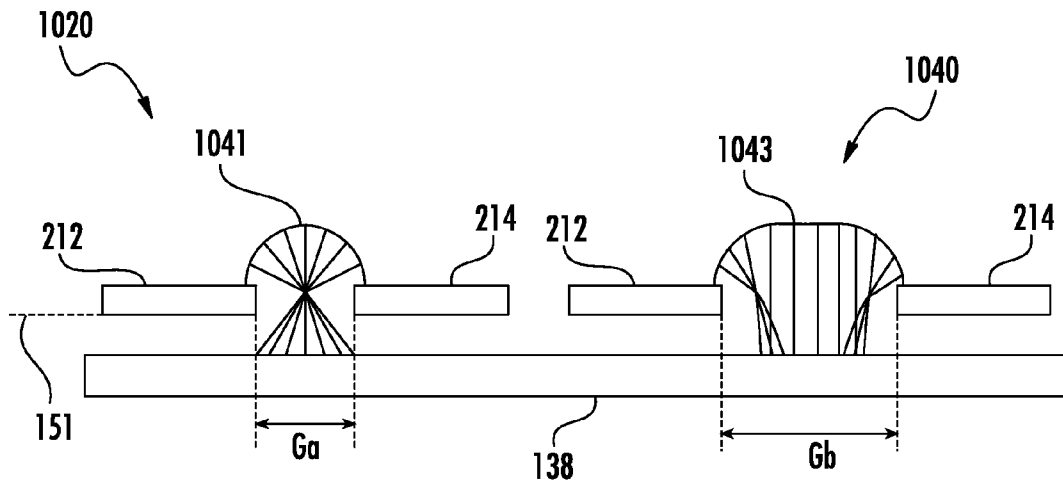


FIG. 10

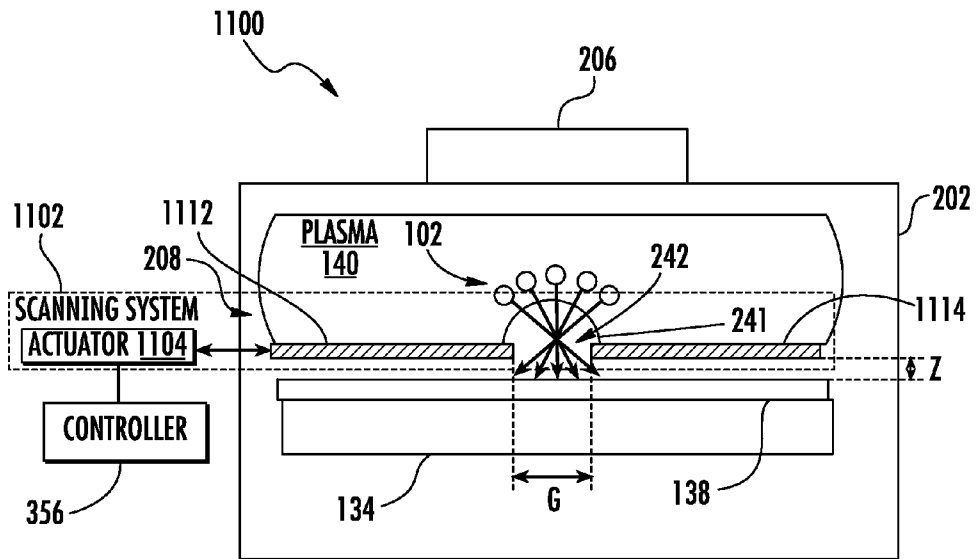


FIG. 11

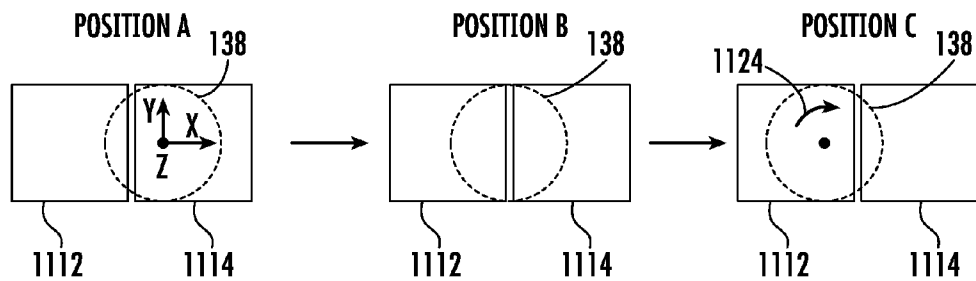


FIG. 12

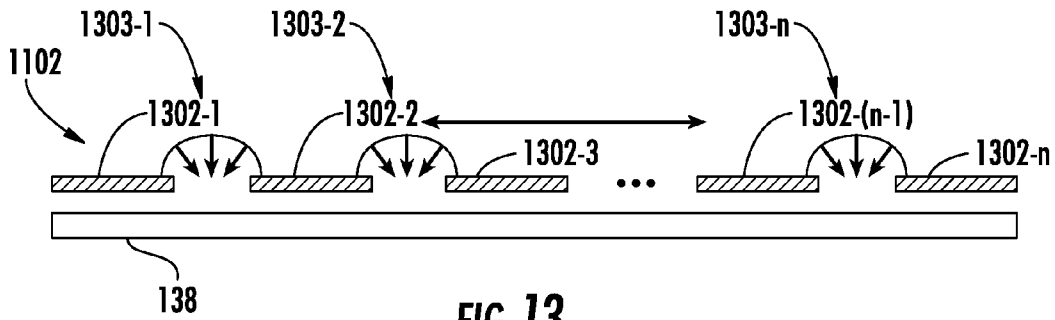


FIG. 13

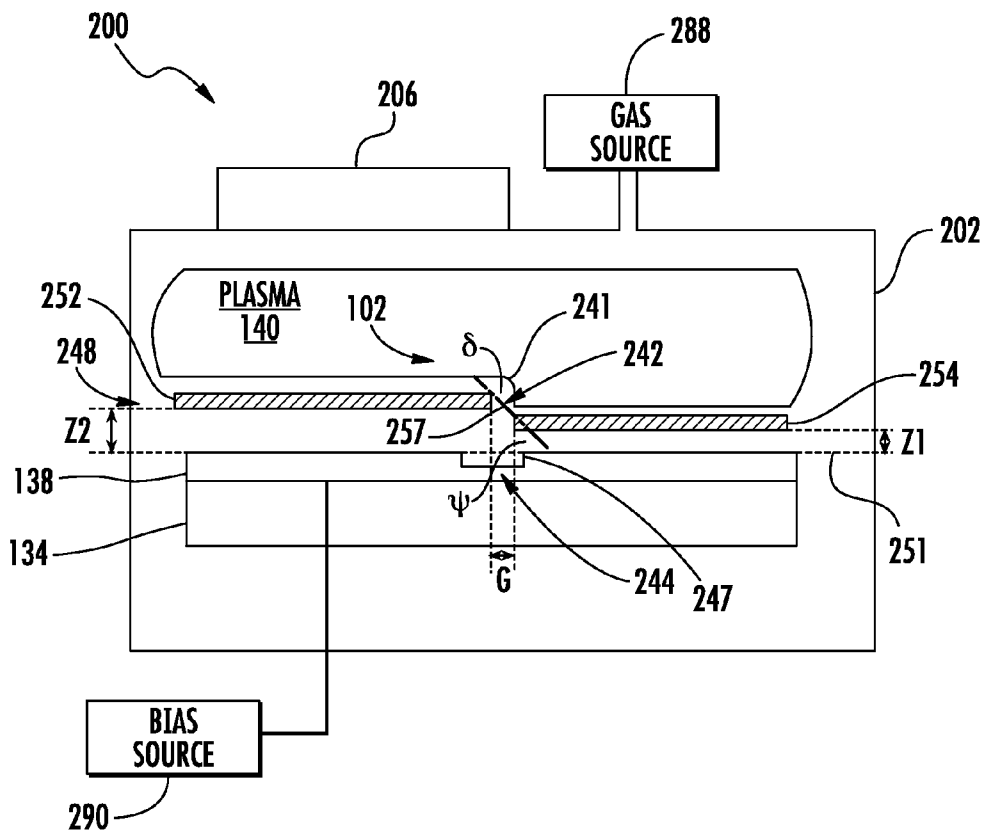


FIG. 14

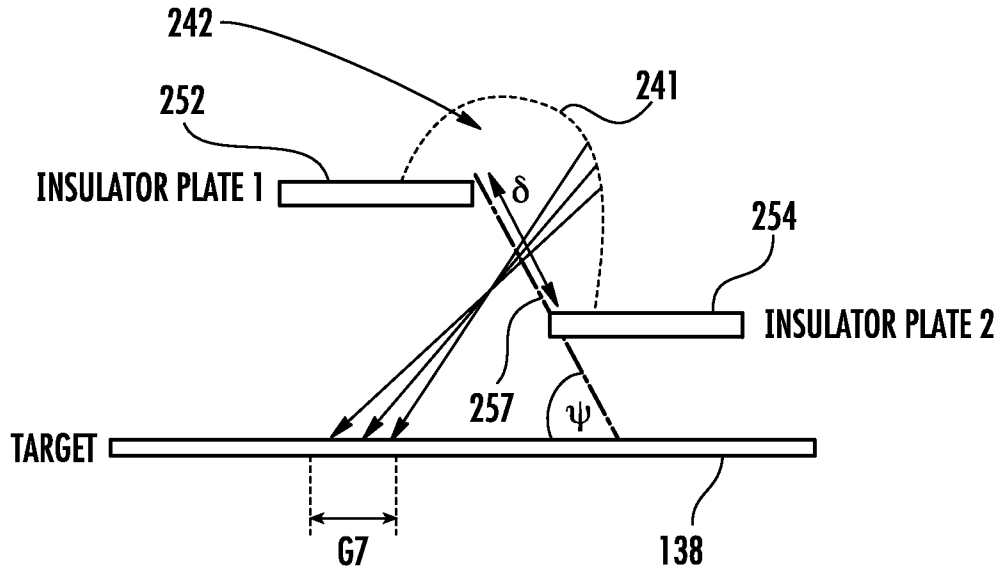


FIG. 15

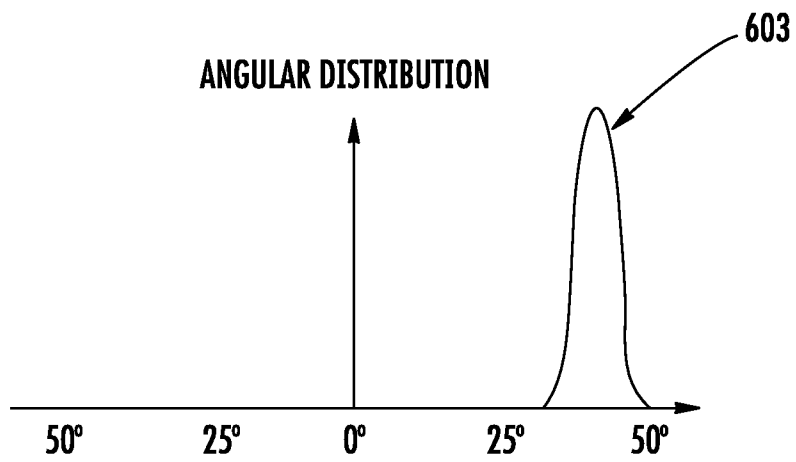


FIG. 16

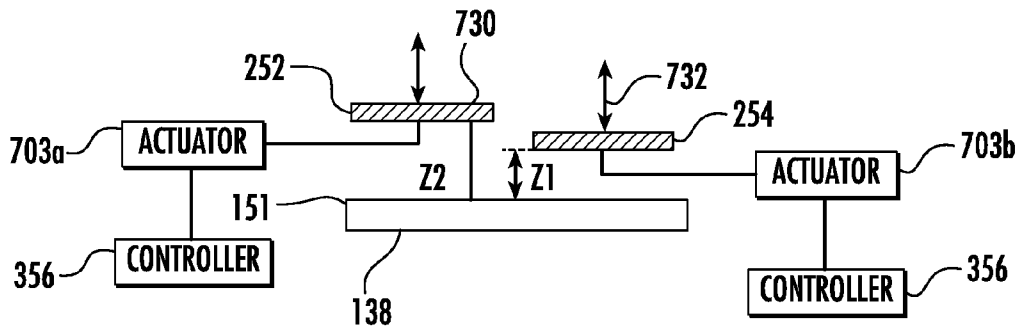


FIG. 17

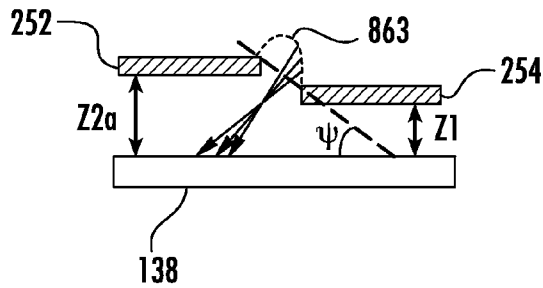


FIG. 18

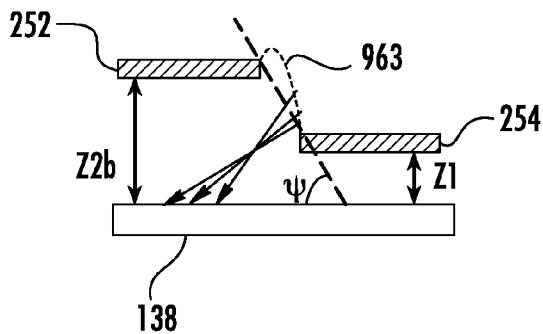


FIG. 19

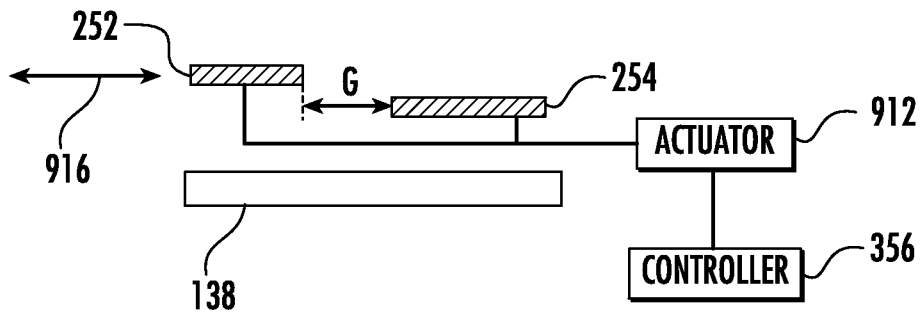


FIG. 20

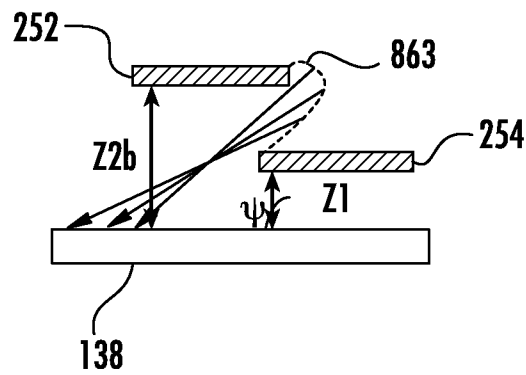


FIG. 21

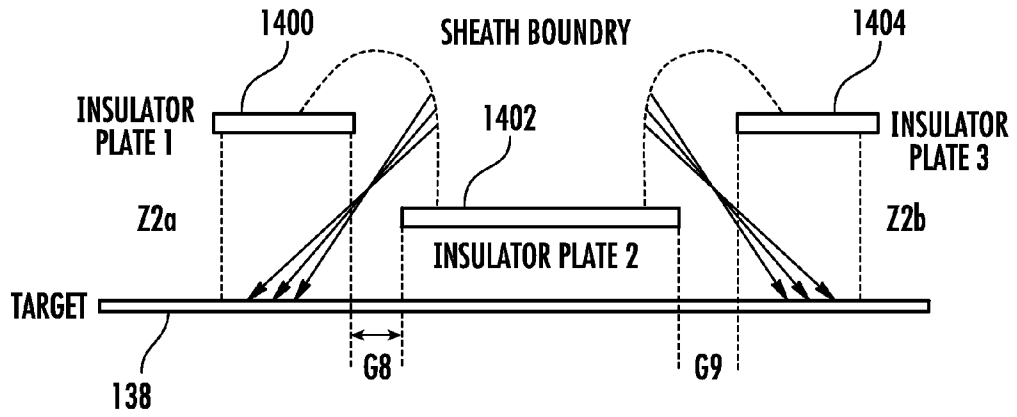


FIG. 22

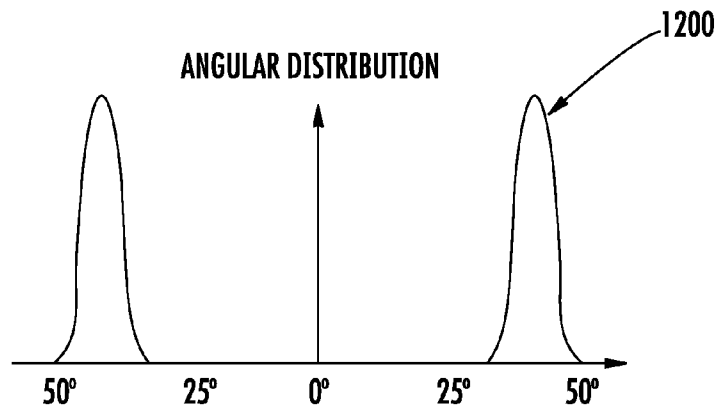


FIG. 23

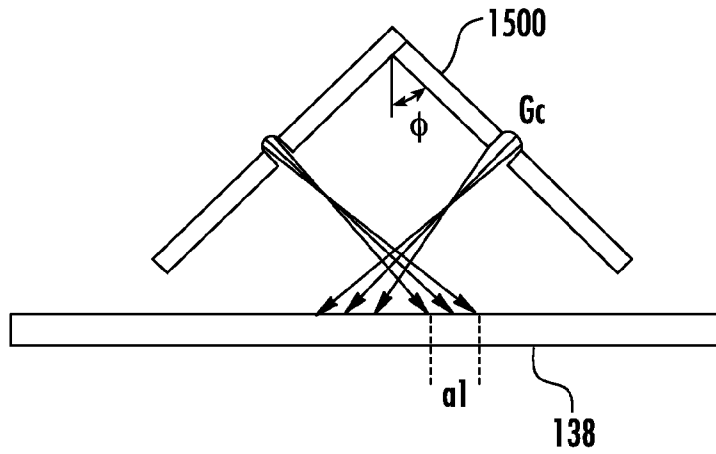


FIG. 24A

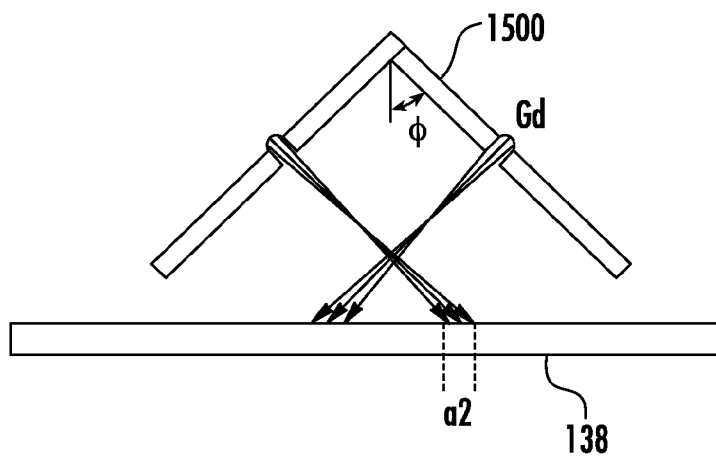


FIG. 24B

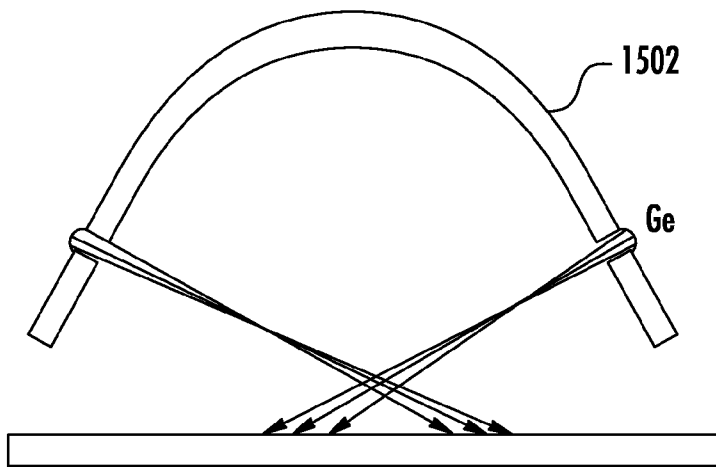


FIG. 24C

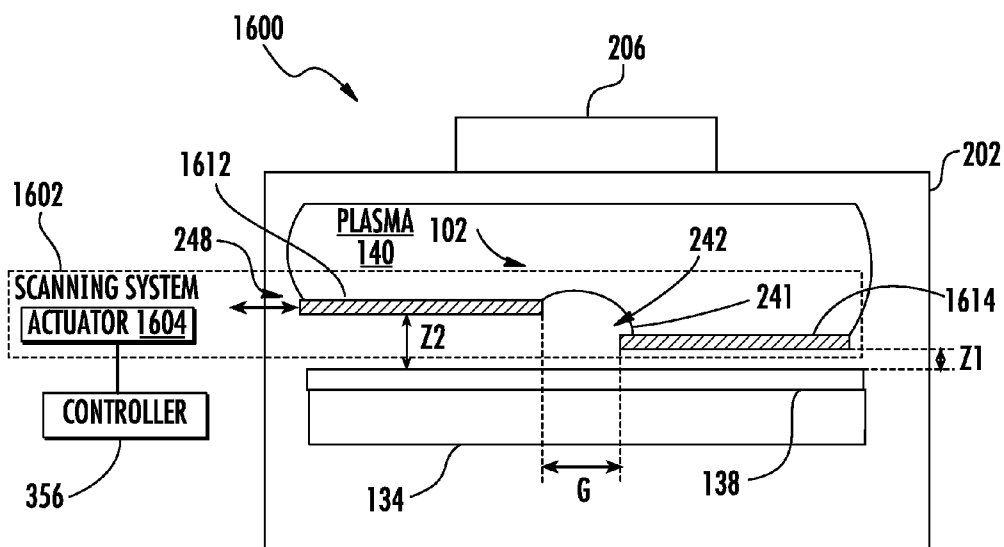


FIG. 25

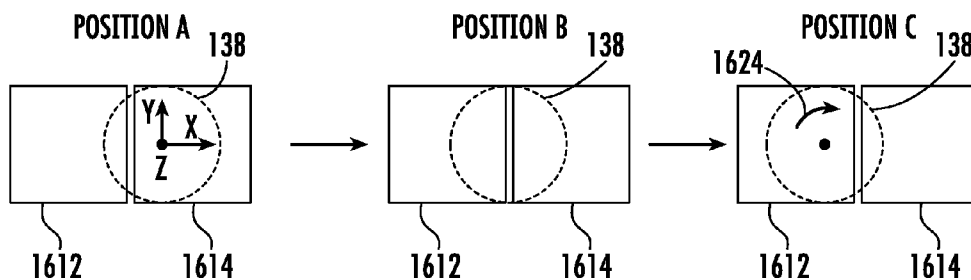


FIG. 26

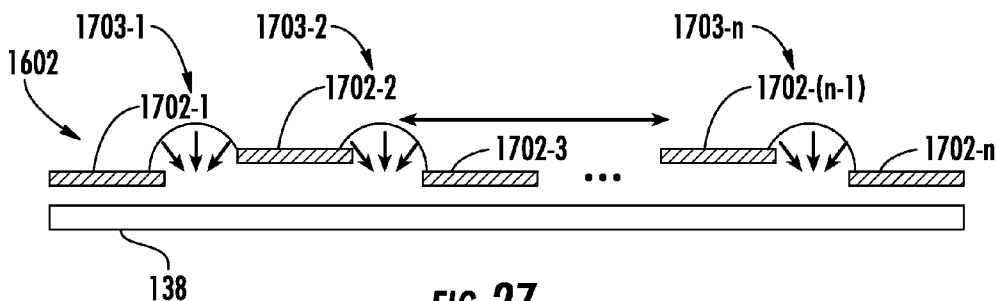


FIG. 27

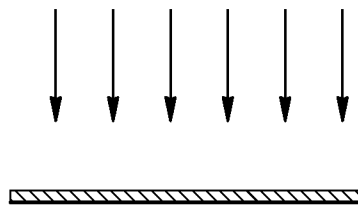


FIG. 28A

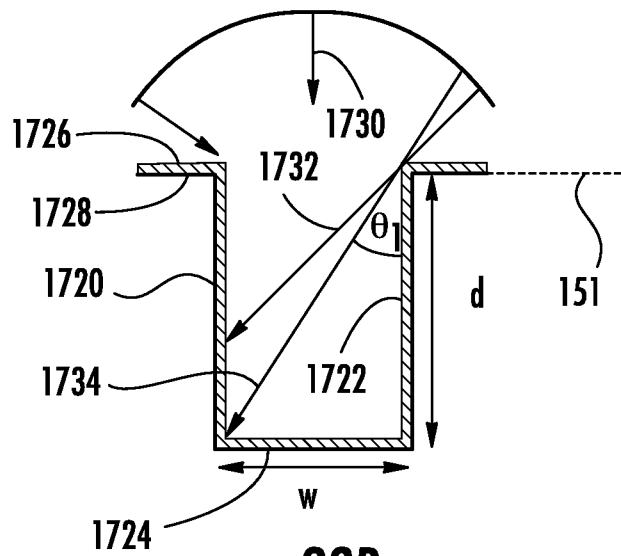


FIG. 28B

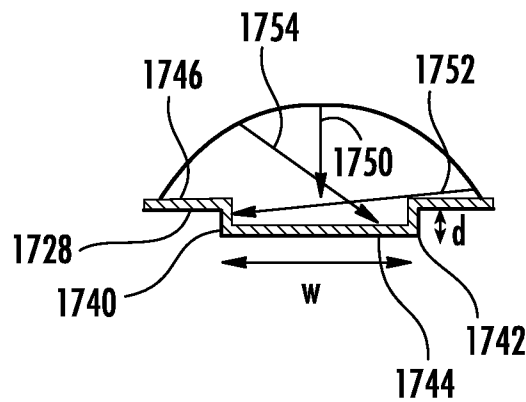


FIG. 28C

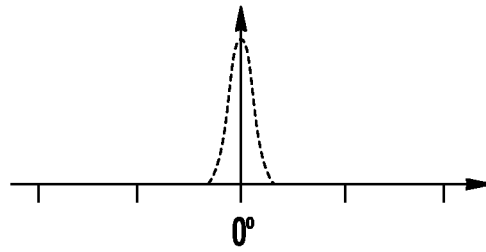


FIG. 29A

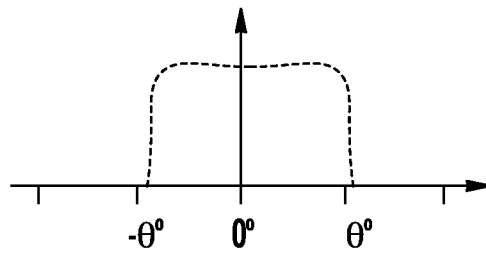


FIG. 29B

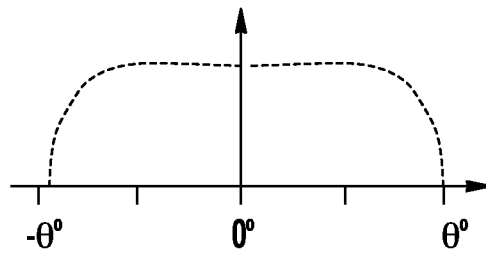


FIG. 29C

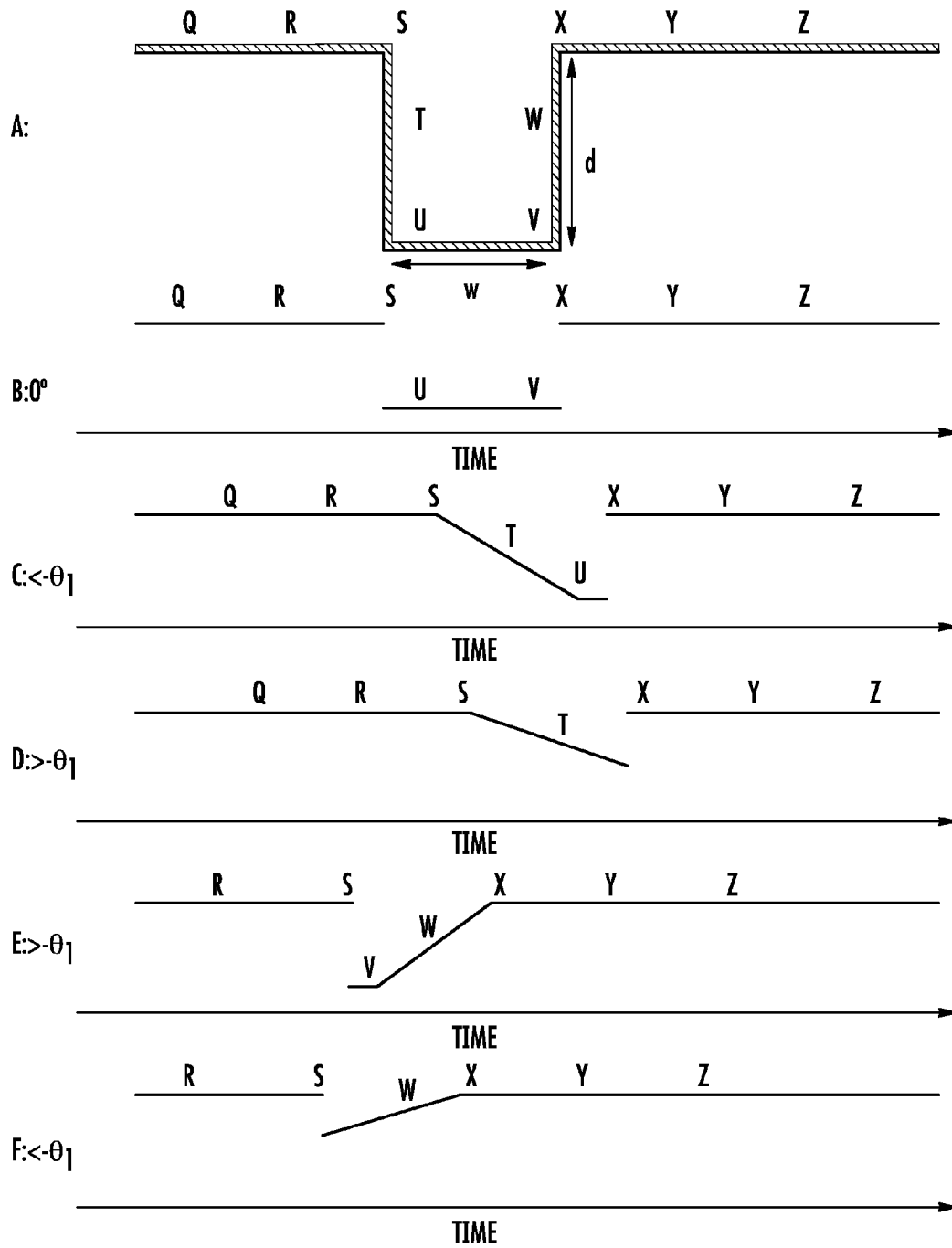


FIG. 30

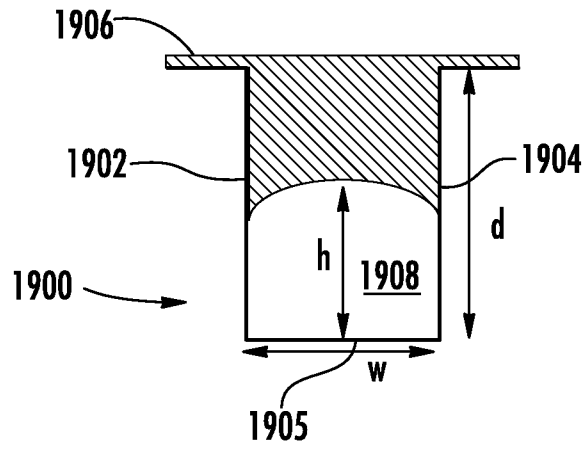


FIG. 31A

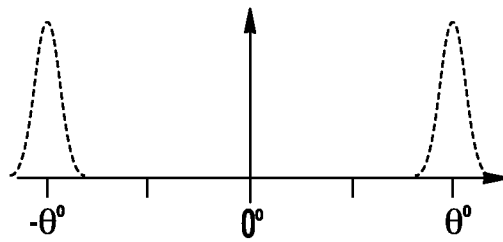


FIG. 31B

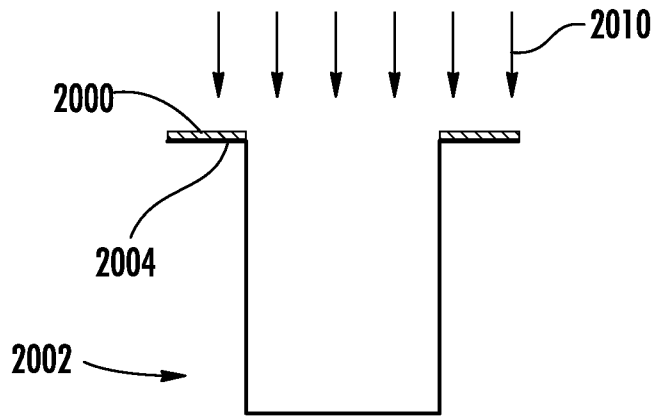


FIG. 32A

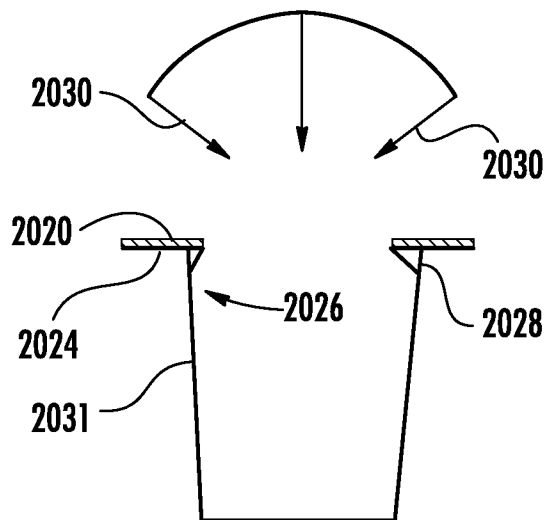


FIG. 32B

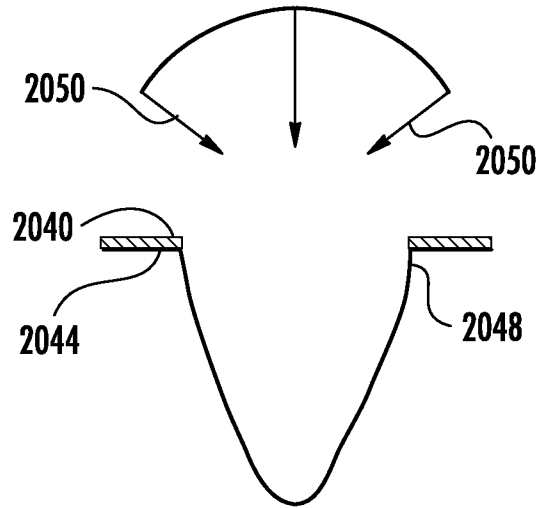


FIG. 32C

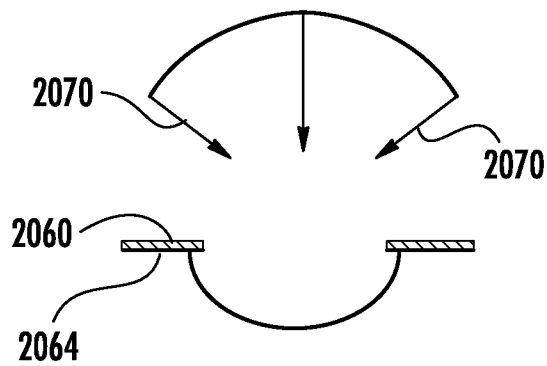


FIG. 32D

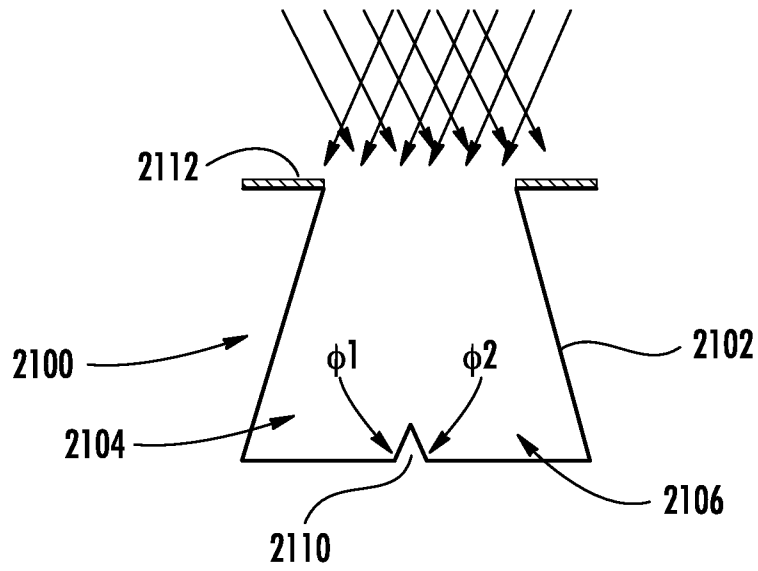


FIG. 33A

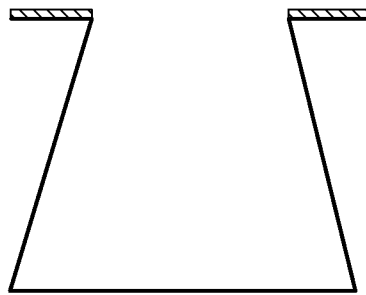


FIG. 33B

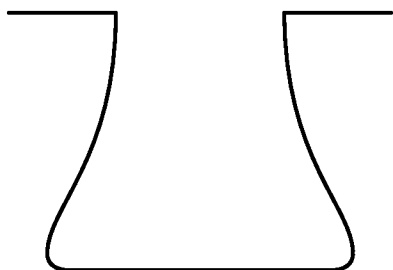


FIG. 33C

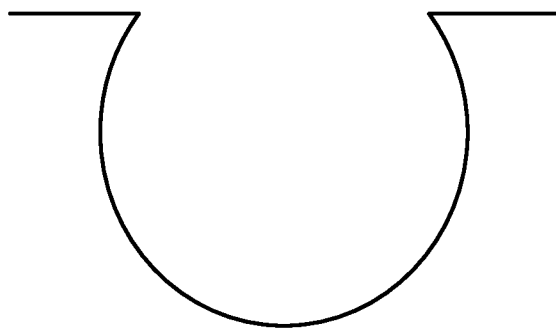


FIG. 33D

ENHANCED ETCH AND DEPOSITION PROFILE CONTROL USING PLASMA SHEATH ENGINEERING

CROSS REFERENCE TO RELATED APPLICATIONS

This application is divisional of prior U.S. application Ser. No. 12/645,638, filed Dec. 23, 2009, which itself is a continuation in part (CIP) of U.S. application Ser. No. 12/644,103, filed Dec. 22, 2009, now U.S. Pat. No. 8,101,510, which itself is a continuation in part (CIP) of U.S. application Ser. No. 12/418,120, filed Apr. 3, 2009, the disclosures of which are incorporated herein by reference.

This application is also related to U.S. application Ser. No. 12/417,929 filed Apr. 3, 2009, now U.S. Pat. No. 7,767,977, which is incorporated herein by reference.

FIELD

This disclosure relates to plasma processing, and more particularly to a plasma processing apparatus.

BACKGROUND

A plasma processing apparatus generates a plasma in a process chamber for treating a workpiece supported by a platen in the process chamber. A plasma processing apparatus may include, but not be limited to, doping systems, etching systems, and deposition systems. The plasma is generally a quasi-neutral collection of ions (usually having a positive charge) and electrons (having a negative charge). The plasma has an electric field of about 0 volts per centimeter in the bulk of the plasma. In some plasma processing apparatus, ions from the plasma are attracted towards a workpiece. In a plasma doping apparatus, ions may be attracted with sufficient energy to be implanted into the physical structure of the workpiece, e.g., a semiconductor substrate in one instance.

The plasma is bounded by a region proximate the workpiece generally referred to as a plasma sheath. The plasma sheath is a region that has fewer electrons than the plasma. The light emission from this plasma sheath is less intense than the plasma since fewer electrons are present and hence few excitation-relaxation collisions occur. Hence, the plasma sheath is sometimes referred to as "dark space."

Turning to FIG. 1, a cross sectional view of portions of a known plasma processing apparatus is illustrated where a plasma 140 has a plasma sheath 142 adjacent to a front surface of a workpiece 138 to be treated. The front surface of the workpiece 138 defines a plane 151, and the workpiece 138 is supported by a platen 134. The boundary 141 between the plasma 140 and the plasma sheath 142 is parallel to the plane 151. Ions 102 from the plasma 140 may be attracted across the plasma sheath 142 towards the workpiece 138. Accordingly, the ions 102 that are accelerated towards the workpiece 138 generally strike the workpiece 138 at about a 0° angle of incidence relative to the plane 151 (e.g., perpendicular to the plane 151). There can be a small angular spread of the angle of incidence of less than about 3°. In addition, by controlling plasma process parameters such as gas pressure within a process chamber, the angular spread may be increased up to about 5°.

A drawback with conventional plasma processing is the lack of angular spread control of the ions 102. As structures on the workpiece become smaller and as three dimensional structures become more common (e.g., trench capacitors, vertical channel transistors such as FinFETs) it would be

beneficial to have greater angle control. For example, a trench 144 having an exaggerated size for clarity of illustration is shown in FIG. 1. With ions 102 being directed at about a 0° angle of incidence or an even angular spread up to 5°, it can be difficult to uniformly treat the sidewalls 147 of the trench 144.

Accordingly, there is a need for a plasma processing apparatus which overcomes the above-described inadequacies and shortcomings.

SUMMARY

The problems of the prior art are overcome by the methods of plasma processing disclosed herein. In certain embodiments, a plasma processing tool is used to deposit material on a workpiece. For example, a method for conformal deposition of material is disclosed. In this embodiment, the plasma sheath shape is modified to allow material to impact the workpiece at a range of incident angles. By varying this range of incident angles over time, a variety of different features can be deposited onto. In another embodiment, a plasma processing tool is used to etch a workpiece. In this embodiment, the plasma sheath shape is altered to allow ions to impact the workpiece at a range of incident angles. By varying this range of incident angles over time, a variety of differently shaped features can be created.

BRIEF DESCRIPTION OF THE DRAWINGS

For a better understanding of the present disclosure, reference is made to the accompanying drawings, in which like elements are referenced with like numerals, and in which:

FIG. 1 is a simplified block diagram of a conventional plasma processing apparatus consistent with the prior art;

FIG. 2 is a block diagram of a plasma processing apparatus consistent with an embodiment of the disclosure;

FIG. 3 is a block diagram of a plasma doping apparatus consistent with an embodiment of the disclosure;

FIG. 4 is a cross sectional view of a pair of insulators to control a shape of a boundary between a plasma and a plasma sheath;

FIG. 5 is a cross sectional view consistent with FIG. 4 illustrating ion trajectories of ions accelerated across the boundary of FIG. 4;

FIG. 6 is a plot of angular ion distributions of the ion trajectories of FIG. 5;

FIG. 7 is a block diagram of a system to control a vertical spacing between a pair of insulators and a workpiece;

FIG. 8 is a cross sectional view consistent with FIG. 7 illustrating ion trajectories at differing vertical spacing;

FIG. 9 is a block diagram of a system to control a horizontal spacing between a pair of insulators;

FIG. 10 is a cross sectional view consistent with FIG. 9 to illustrating ion trajectories at differing horizontal spacing;

FIG. 11 is a block diagram of a plasma processing apparatus having a scanning system to move a pair of insulating sheets relative to a workpiece;

FIG. 12 is a plan view of the insulating sheets of FIG. 11 showing relative movement between the insulating sheets and a disk shaped workpiece;

FIG. 13 is a block diagram of a scanning system consistent with FIG. 11 having a plurality of insulators;

FIG. 14 is a block diagram of a plasma processing apparatus consistent with a second embodiment of the disclosure;

FIG. 15 is a cross sectional view of two insulators used to control a shape of a boundary between a plasma and a plasma sheath;

FIG. 16 is a plot of angular ion distributions of the ion trajectories of FIG. 15;

FIG. 17 is a block diagram of a system to control a vertical spacing between a set of insulators and a workpiece;

FIG. 18 is a cross sectional view consistent with FIG. 17 illustrating ion trajectories at a first vertical spacing;

FIG. 19 is a cross sectional view consistent with FIG. 17 illustrating ion trajectories at a second vertical spacing;

FIG. 20 is a block diagram of a system to control a horizontal spacing between insulators;

FIG. 21 is a cross sectional view consistent with FIG. 20 illustrating ion trajectories at negative horizontal spacing;

FIG. 22 is a cross sectional view of three insulators used to control a shape of a boundary between a plasma and a plasma sheath;

FIG. 23 is a plot of angular ion distributions of the ion trajectories of FIG. 22;

FIGS. 24a-c are cross sectional views of additional embodiments of the insulating modifier;

FIG. 25 is a block diagram of a plasma processing apparatus having a scanning system to move insulating sheets relative to a workpiece;

FIG. 26 is a plan view of the insulating sheets of FIG. 25 showing relative movement between the insulating sheets and a disk shaped workpiece;

FIG. 27 is a block diagram of a scanning system consistent with FIG. 25 having a plurality of insulators;

FIG. 28a illustrates the traditional path of ions from a plasma to a workpiece;

FIG. 28b illustrates the conformal deposition of a narrow three dimensional feature;

FIG. 28c illustrates the conformal deposition of a wide, shallow three dimensional feature;

FIG. 29a shows the ion angular distribution associated with FIG. 28a;

FIG. 29b shows the ion angular distribution associated with FIG. 28b;

FIG. 29c shows the ion angular distribution associated with FIG. 28c;

FIGS. 30a-f show the effects of various angles of incidence on deposition;

FIG. 31a illustrates the depositing of material with an air gap in a three dimensional feature;

FIG. 31b shows the ion angular distribution associated with FIG. 30a;

FIG. 32a illustrates the etching of a three-dimensional feature with vertical sidewalls;

FIG. 32b illustrates the etching of a three-dimensional feature with inwardly tapered sidewalls;

FIG. 32c illustrates a feature shape that can be created using the ion angular distribution of FIG. 29b;

FIG. 32d illustrates a feature shape that can be created using the ion angular distribution of FIG. 29c;

FIG. 33a illustrates the etching of a three-dimensional feature with outwardly tapered sidewalls;

FIG. 33b illustrates a feature shape that can be created using the ion angular distribution of FIG. 30b;

FIG. 33c illustrates a feature shape that can be created using the ion angular distribution of FIG. 30b; and

FIG. 33d illustrates a feature shape that can be created using the ion angular distribution of FIG. 30b.

DETAILED DESCRIPTION

FIG. 2 is a block diagram of one plasma processing apparatus 200 having an insulating modifier 208 consistent with an embodiment of the disclosure. The insulating modifier 208 is

configured to modify an electric field within the plasma sheath 242 to control a shape of a boundary 241 between the plasma 140 and the plasma sheath 242. Accordingly, ions 102 that are attracted from the plasma 140 across the plasma sheath 242 may strike the workpiece 138 at a range of incident angles.

The plasma processing apparatus 200 may be further described herein as a plasma doping apparatus. However, the plasma processing apparatus 200 may also include, but not be limited to, etching and deposition systems. Furthermore, a plasma doping system can perform many differing material modification processes on a treated workpiece. One such process includes doping a workpiece, such as a semiconductor substrate, with a desired dopant.

The plasma processing apparatus 200 may include a process chamber 202, a platen 134, a source 206, and the insulating modifier 208. The platen 134 is positioned in the process chamber 202 for supporting the workpiece 138. The workpiece may include, but not be limited to, a semiconductor wafer, flat panel, solar panel, and polymer substrate. The semiconductor wafer may have a disk shape with a diameter of 300 millimeters (mm) in one embodiment. The source 206 is configured to generate the plasma 140 in the process chamber 202 as is known in the art. In the embodiment of FIG. 2, the insulating modifier 208 includes a pair of insulators 212 and 214 defining a gap there between having a horizontal spacing (G). In other embodiments, the insulating modifier may include only one insulator. The pair of insulators 212 and 214 may be a pair of sheets having a thin, flat shape. In other embodiments, the pair of insulators 212 and 214 may be other shapes such as tube shaped, wedge shaped, and/or have a beveled edge proximate the gap.

In one embodiment, the horizontal spacing of the gap defined by the pair of insulators 212 and 214 may be about 6.0 millimeters (mm). The pair of insulators 212 and 214 may also be positioned a vertical spacing (Z) above the plane 151 defined by the front surface of the workpiece 138. In one embodiment, the vertical spacing (Z) may be about 3.0 mm.

In operation, a gas source 288 supplies an ionizable gas to the process chamber 202. Examples of an ionizable gas include, but are not limited to, BF_3 , BI_3 , N_2 , Ar, PH_3 , AsH_3 , B_2H_6 , H_2 , Xe, Kr, Ne, He, SiH_4 , SiF_4 , GeH_4 , GeF_4 , CH_4 , CF_4 , AsF_5 , PF_3 , and PF_5 . The source 206 may generate the plasma 140 by exciting and ionizing the gas provided to the process chamber 202. Ions may be attracted from the plasma 140 across the plasma sheath 242 by different mechanisms. In the embodiment of FIG. 2, the bias source 290 is configured to bias the workpiece 138 to attract ions 102 from the plasma 140 across the plasma sheath 242. The bias source 290 may be a DC power supply to provide a DC voltage bias signal or an RF power supply to provide an RF bias signal.

Advantageously, the insulating modifier 208 modifies the electric field within the plasma sheath 242 to control a shape of the boundary 241 between the plasma 140 and the plasma sheath 242. In the embodiment of FIG. 2, the insulating modifier 208 includes a pair of insulators 212 and 214. The insulators 212, 214 may be fabricated of quartz, alumina, boron nitride, glass, silicon nitride, etc. The boundary 241 between the plasma 140 and the plasma sheath 242 may have a convex shape relative to the plane 151. When the bias source 290 biases the workpiece 138, ions 102 are attracted across the plasma sheath 242 through the gap between the insulators 212 and 214 at a large range of incident angles. For instance, ions following trajectory path 271 may strike the workpiece 138 at an angle of $+0^\circ$ relative to the plane 151. Ions following trajectory path 270 may strike the workpiece 138 at about an angle of 0° relative to the same plane 151. Ions following

trajectory path 269 may strike the workpiece 138 an angle of $-\theta^\circ$ relative to the plane 151. Accordingly, the range of incident angles may be between $+\theta^\circ$ and $-\theta^\circ$ centered about 0° . In addition, some ion trajectories paths such as paths 269 and 271 may cross each other. Depending on a number of factors including, but not limited to, the horizontal spacing (G) between the insulators 212 and 214, the vertical spacing (Z) of the insulators above the plane 151, the dielectric constant of the insulators 212 and 214, and other plasma process parameters, the range of incident angles (θ) may be between $+60^\circ$ and -60° centered about 0° . Hence, small three dimensional structures on the workpiece 138 may be treated uniformly by the ions 102. For example, the sidewalls 247 of the trench 244 having an exaggerated size for clarity of illustration may be more uniformly treated by the ions 102 compared to that of FIG. 1.

Turning to FIG. 3, a block diagram of one exemplary plasma doping apparatus 300 is illustrated. Consistent with the apparatus of FIG. 2, the plasma doping apparatus 300 has the pair of insulators 212 and 214 to control a shape of the boundary 241 between the plasma 140 and the plasma sheath 242.

The plasma doping apparatus 300 includes a process chamber 202 defining an enclosed volume 303. A gas source 304 provides a primary dopant gas to the enclosed volume 303 of the process chamber 302 through the mass flow controller 306. A gas baffle 370 may be positioned in the process chamber 202 to deflect the flow of gas from the gas source 304. A pressure gauge 308 measures the pressure inside the process chamber 202. A vacuum pump 312 evacuates exhausts from the process chamber 202 through an exhaust port 310. An exhaust valve 314 controls the exhaust conductance through the exhaust port 310.

The plasma doping apparatus 300 may further includes a gas pressure controller 316 that is electrically connected to the mass flow controller 306, the pressure gauge 308, and the exhaust valve 314. The gas pressure controller 316 may be configured to maintain a desired pressure in the process chamber 202 by controlling either the exhaust conductance with the exhaust valve 314 or a process gas flow rate with the mass flow controller 306 in a feedback loop that is responsive to the pressure gauge 308.

The process chamber 202 may have a chamber top 318 that includes a first section 320 formed of a dielectric material that extends in a generally horizontal direction. The chamber top 318 also includes a second section 322 formed of a dielectric material that extends a height from the first section 320 in a generally vertical direction. The chamber top 318 further includes a lid 324 formed of an electrically and thermally conductive material that extends across the second section 322 in a horizontal direction.

The plasma doping apparatus further includes a source 301 configured to generate a plasma 140 within the process chamber 202. The source 301 may include a RF source 350 such as a power supply to supply RF power to either one or both of the planar antenna 326 and the helical antenna 346 to generate the plasma 140. The RF source 350 may be coupled to the antennas 326, 346 by an impedance matching network 352 that matches the output impedance of the RF source 350 to the impedance of the RF antennas 326, 346 in order to maximize the power transferred from the RF source 350 to the RF antennas 326, 346.

The plasma doping apparatus may also include a bias power supply 390 electrically coupled to the platen 134. The plasma doping system may further include a controller 356 and a user interface system 358. The controller 356 can be or include a general-purpose computer or network of general-

purpose computers that may be programmed to perform desired input/output functions. The controller 356 may also include communication devices, data storage devices, and software. The user interface system 358 may include devices such as touch screens, keyboards, user pointing devices, displays, printers, etc. to allow a user to input commands and/or data and/or to monitor the plasma doping apparatus via the controller 356. A shield ring 394 may be disposed around the platen 134 to improve the uniformity of implanted ion distribution near the edge of the workpiece 138. One or more Faraday sensors such as Faraday cup 399 may also be positioned in the shield ring 394 to sense ion beam current.

In operation, the gas source 304 supplies a primary dopant gas containing a desired dopant for implantation into the workpiece 138. The source 301 is configured to generate the plasma 140 within the process chamber 302. The source 301 may be controlled by the controller 356. To generate the plasma 140, the RF source 350 resonates RF currents in at least one of the RF antennas 326, 346 to produce an oscillating magnetic field. The oscillating magnetic field induces RF currents into the process chamber 202. The RF currents in the process chamber 202 excite and ionize the primary dopant gas to generate the plasma 140.

The bias power supply 390 provides a pulsed platen signal having a pulse ON and OFF periods to bias the platen 134 and hence the workpiece 138 to accelerate ions from the plasma 140 towards the workpiece 138 across the plasma sheath 242. The ions 102 may be positively charged ions and hence the pulse ON periods of the pulsed platen signal may be negative voltage pulses with respect to the process chamber 202 to attract the positively charged ions 102. The frequency of the pulsed platen signal and/or the duty cycle of the pulses may be selected to provide a desired dose rate. The amplitude of the pulsed platen signal may be selected to provide a desired energy.

Advantageously, the pair of insulators 212 and 214 controls the shape of the boundary 241 between the plasma 140 and the plasma sheath 242 as previously detailed with respect to FIG. 2. Therefore, the ions 102 may be attracted across the plasma sheath 242 through the gap between the insulators 212 and 214 at a large range of incident angles for doping the workpiece 138.

Turning to FIG. 4, a partial cross sectional view of the pair of insulators 212 and 214 and workpiece 138 is illustrated showing the electric field lines in the plasma sheath 242 about the gap defined by the insulators 212 and 214. The electric field lines and resulting arcuate boundary 241 between the plasma and the plasma sheath 242 resulted from a computer simulation with the workpiece 138 biased at $-2,000$ volts and the insulators 212 and 214 fabricated of glass. As illustrated, the arcuate boundary 241 about the gap may further have a convex shape relative to the plane 151.

FIG. 5 is a cross sectional view consistent with FIG. 4 illustrating simulated ion trajectories accelerated across the plasma sheath 242 through the gap between the insulators 212 and 214. In a plasma doping apparatus, the ions may be implanted in the workpiece 138 in a central area of the gap spacing due to the shape of the boundary 241 and the electric field lines within the plasma sheath 242. For instance, of the total horizontal spacing (G1) between the insulators 212 and 214, ions strike the workpiece 138 about the central horizontal spacing (G3). No ions strike the workpiece about the peripheral horizontal spacing (G2) and (G4) proximate the insulators 212 and 214 in this embodiment.

FIG. 6 is a plot 602 of the distribution of incident angles of ions striking the workpiece 138 consistent with the illustrated ion trajectories of FIG. 5. As shown, the plot 602 reveals the

incident angles are centered about 0° and vary over a large range of angles from about $+60^\circ$ to -60° . This large range of incident angles enables conformal doping of three dimensional structures. For example, the sidewalls of a trench structure may be more uniformly doped with ions having such a large range of incident angles.

Turning to FIG. 7, a block diagram of another embodiment consistent with the present disclosure is illustrated where the vertical spacing (Z) between an insulating modifier and the plane 151 defined by the front surface of the workpiece 138 may be adjusted. The insulating modifier may be the pair of insulators 212 and 214 as detailed in other embodiments. An actuator 702 may be mechanically coupled to the pair of insulators 212 and 214 to drive the insulators in a vertical direction as shown by arrows 720, 722 relative to the plane 151. The Z position of the pair of insulators 212 and 214 relative to the plane 151, and also relative to each other, influences the shape of the boundary between the plasma and the plasma sheath and also the trajectories of the ions striking the workpiece 138. The actuator 702 may be controlled by a controller such as controller 356.

FIG. 8 is a cross sectional view consistent with FIG. 7 to illustrate ion trajectories at differing Z positions of the pair of insulators 212 and 214 relative to the plane 151 with all other parameters being equal. In the first relatively short Z gap position 820, the insulators 212, 214 are positioned a first distance (Z1) above the plane 151. In a comparatively taller Z gap position 840, the insulators 212, 214 are positioned a second distance (Z2) above the plane 151, where $(Z2) > (Z1)$. In the first position 820, the boundary 841 between the plasma and the plasma sheath has a convex shape relative to the plane 151. The boundary 841 also has a shape that approximately approaches the shape of a portion of a circumference of a circle where an apex of the arcuate shape is a distance (Za) above a top surface of the insulator 212. In contrast, the boundary 843 in the second position 840 has a shallower shape where the apex of the arcuate shape is a shorter distance (Zb) above the top surface of the insulator 212, or where $(Zb) < (Za)$. The shape of the boundaries 841, 843 combined with the Z gap distances (Z1) and (Z2) and the electric field lines in the plasma sheath, influences the angular spread of the ions striking the workpiece 138. For example, the angular spread of ions striking the workpiece 138 with the relatively short Z gap position 820 is greater than the angular spread of ions striking the workpiece 138 with the relatively longer Z gap position. In addition, ions strike a wider horizontal spacing (G5) of the workpiece 138 with the shorter Z gap position 820 compared to the horizontal spacing (G6) with the taller Z gap position, where $(G6) < (G5)$. Although not illustrated in FIG. 8, the Z gap positions of each insulator 212 and 214 may also be different from each other to further influence the shape of the boundary between the plasma and the plasma sheath and accordingly the angular spread of ions.

Turning to FIG. 9, a block diagram of another embodiment consistent with the present disclosure is illustrated where the horizontal spacing (G) between insulators 212 and 214 may be adjusted. The horizontal spacing adjustments may in lieu of, or in addition to, the earlier detailed vertical spacing adjustments of FIGS. 8 and 9. An actuator 902 may be mechanically coupled to at least one of the pair of insulators 212 and 214 to drive the insulators in the direction shown by the arrow 906 relative to one another. The actuator 902 may be controlled by a controller such as controller 356.

FIG. 10 is a cross sectional view consistent with FIG. 9 to illustrate ion trajectories at differing horizontal gap spacing between the insulators 212 and 214 with all other parameters being equal. In the first relatively shorter horizontal gap posi-

tion 1020, the insulators 212, 214 are positioned a first horizontal distance (Ga) from one another. In a comparatively longer horizontal gap position 1040, the insulators 212, 214 are positioned a second horizontal distance (Gb) from each other, where $(Gb) > (Ga)$. In the first position 1020, the boundary 1041 between the plasma and the plasma sheath has a convex shape relative to the plane 151. The boundary 1041 also has a shape that approximately approaches the shape of a portion of a circumference of a circle. In contrast, the boundary 1043 in the second position 1040 has a convex shape relative to the plane 151 where a central portion of the boundary 1043 is about parallel to the plane 151. As a result, a larger corresponding central portion of the workpiece 138 is struck with ions having about a 0° angle of incidence relative to the plane 151.

FIG. 11 is a block diagram of a plasma processing apparatus 1100 having a scanning system 1102 to drive an insulating modifier 208 relative the workpiece 138. In the embodiment of FIG. 11, the insulating modifier 208 includes a pair of square insulating sheets 1112 and 1114 that are best seen in FIG. 12. The scanning system 1102 may include an actuator 1104 mechanically coupled to the insulating sheets 1112 and 1114 to drive the same. The actuator 1104 may be controlled by a controller such as controller 356.

FIG. 12 is plan view of the square insulating sheets 1112 and 1114 and a disk shaped workpiece 138 to illustrate one example of relative movement between the same. In the embodiment of FIG. 12, the scanning system 1102 may drive the square insulating sheets 1112 and 1114 from Position A, to Position B, and Position C, etc. so that all portions of the workpiece 138 are exposed to the gap defined by the pair of square insulating sheets 1112 and 1114. If a Cartesian coordinate system is defined as detailed in FIG. 12, the insulating sheets 1112 and 1114 are driven in the X direction of FIG. 12. In other embodiments, the insulating sheets 1112 and 1114 or another set of different insulating sheets may be driven in the Y direction or any angle between the X and Y directions. In addition, the workpiece 138 may be rotated as the scanning system 1102 drives the insulating sheets 1112 and 1114 in one direction. The workpiece 138 may also be rotated by a predetermined rotation angle after the scanning system 1102 drives the insulating sheets in one direction. In one example, the rotation may be about a central axis of the workpiece as illustrated by arrow 1124.

Turning to FIG. 13, a scanning system 1102 consistent with FIG. 11 is illustrated. Compared to FIG. 11, the scanning system 1102 of FIG. 13 includes a plurality of insulators 1302-1, 1302-2, 1302-3, . . . 1302-(n-1), and 1302-n that define a plurality of gaps there between 1303-1, 1303-2, . . . 1303-n. The scanning system may drive the plurality of insulators 1302-1, 1302-2, 1302-3, . . . 1302-(n-1), and 1302-n relative to the workpiece 138 so the plurality of gaps 1303-1, 1303-2, . . . 1303-n pass over the workpiece 138.

FIG. 14 shows a second embodiment of the plasma processing apparatus of FIG. 2. As described above, the plasma processing apparatus 200 may include a process chamber 202, a platen 134, a source 206, and the insulating modifier 248. In the embodiment of FIG. 14, the insulating modifier 248 includes insulators 252 and 254 defining a gap there between having a horizontal spacing (G). In other embodiments, the insulating modifier 248 may include only one insulator. In one embodiment, the horizontal spacing of the gap defined by the insulators 252 and 254 may be between about 1 and 60 millimeters (mm), depending on the sheath thickness and the desired angular distribution.

The insulators 252 and 254 may also be positioned a vertical spacing (Z1,Z2) above the plane 151 defined by the front

surface of the workpiece **138**. In one embodiment, the closer vertical spacing (**Z1**) may be between about 1 and 10 mm. In some embodiments, the difference in height between the insulators (i.e. **Z2-Z1**) may be between about 0 and 40 mm, depending on the sheath thickness and the desired angular distribution. While FIG. **14** shows insulator **252** at a greater vertical height than insulator **254**, the insulator **254** may have a greater vertical height than insulator **252** if desired.

The difference in vertical height between the two insulators creates a gap angle, relative to plane **151**. The gap angle is measured by creating a plane **257**, which passes through the edges of insulator **252** closest to the sheath and proximate the gap and the edges of insulator **254** closest to the sheath and proximate the gap. The angle between plane **257** and plane **151** defines the gap angle (ψ). In some embodiments, the gap width (δ) is measured along plane **257**, rather than along the horizontal. The gap width (δ) is related to the horizontal spacing (**G**) according to the equation:

$$\delta = G / \cos(\psi),$$

where ψ is the gap angle. The gap width (δ) may be between 0 and 40 mm. In some embodiments, the horizontal spacing may be 0 or even negative (which is achieved when the insulators overlap one another). A large difference in **Z2-Z1**, coupled with a 0 mm or negative horizontal spacing can be used to create very large center angles, such as greater than 80°.

As will be described in more detail below, the disclosed apparatus can be used to create angular distributions of ions. These angular distributions, such as those shown in FIGS. **16** and **23**, can be characterized by two parameters. The first is the center angle, which is the angle that forms the center of the angular distribution. The center angle is defined as the angular deviation from the orthogonal to plane **151**. In other words, ions that strike perpendicular to the plane **151** at said to have a center angle of 0°. As the angle of incidence become more parallel to plane **151**, its value increases.

In FIG. **16**, the center angle corresponds to about 45°. In FIG. **23**, there are two center angles, at -45° and +45°. The second parameter of interest is the angular spread, or angular range. This is the distribution of ions about the center angle. In other words, all ions do not strike the workpiece at the same angle. Rather, they arrive having an angular distribution about the center angle. In FIG. **16**, the distribution of angles is roughly from 35° to 55°; thereby having an angular spread (or range) of about 20°. Similarly, the angular spread (or angular distribution) of FIG. **23** is about 20°.

The gap angle (ψ) helps to define the center angle. To create a center angle that is not perpendicular to the workpiece plane **151** (i.e. a non-zero center angle), the gap angle (ψ) may be non-zero. In other words, a non-zero gap angle (ψ) implies that the gap plane **257** is not parallel to the workpiece plane **151**. By having a non-zero gap angle (ψ), the center angle is changed so as not to be perpendicular to the workpiece plane **151**. Larger gap angles (i.e. >30°) typically create larger deviations in the center angle (i.e. >30°). Smaller gap angles (i.e. when the gap plane **257** and the workpiece plane **151** are nearly parallel) produce smaller center angles (i.e. <10°).

The boundary **241** between the plasma **140** and the plasma sheath **242** may have an irregular shape relative to the plane **151**. When the bias source **290** biases the workpiece **138**, ions **102** are attracted across the plasma sheath **242** through the gap between the insulators **252** and **254** at a large range of center angles. For instance, ions may strike the workpiece **138** at a non-zero center angle of + θ° relative to the plane **151**. If the vertical spacing of the insulators is reversed, ions may strike the workpiece **138** a non-zero center angle of - θ°

relative to the plane **151**. Accordingly, the range of incident angles may be centered about θ° , where θ is between -80° and 80°. Depending on a number of factors including, but not limited to, the horizontal spacing (**G**) between the insulators **252** and **254**, the vertical spacing (**Z1**, **Z2**) of the insulators above the plane **151**, the gap width (δ), the gap angle (ψ), the difference in vertical spacing (**Z2-Z1**), the dielectric constant of the insulators **252** and **254**, the dielectric thickness of the insulators **252** and **254**, and other plasma process parameters, the range and center of the incident angles (θ) may be modified. For example, the angular distribution may be between +5 degrees and -5 degrees, while the center angle can be between -80° and +80°. In other embodiments, the angular distribution may be greater (or smaller). Similarly, the center angle can be modified to achieve other values. Hence, small three dimensional structures on the workpiece **138** may be treated uniformly by the ions **102**.

FIG. **15** is a cross sectional view illustrating simulated ion trajectories accelerated across the plasma sheath **242** through the gap between the insulators **252** and **254**. In a plasma doping apparatus, the ions may be implanted in the workpiece **138** in a central area of the gap spacing due to the shape of the boundary **241** and the electric field lines within the plasma sheath **242**. For instance, due to the difference in vertical spacing between the two insulators **252**, **254**, ions strike the workpiece at a non-zero angle in the space (**G7**). In addition, few ions strike the workpiece proximate the insulators outside of space **G7** in this embodiment.

FIG. **16** is a plot **603** of the distribution of incident angles of ions striking the workpiece **138** consistent with the illustrated ion trajectories of FIG. **15**. As shown, the plot **603** reveals the incident angles are centered about a non-zero center angle of about 45 degrees with an angular distribution of about 20 degrees about this center angle. In other embodiments, the center angle can vary between -80 to +80 degrees and the angular distribution about the center angle may vary from about +20 to -20 degrees. This range of incident angles enables conformal doping of three dimensional structures.

By varying the gap width (δ), the spacing between the insulators (**Z2-Z1**) and the position of the insulators with respect to the workpiece (**Z1**), the center angle and angular distribution can be modified to achieve a wide range of values, including, but not limited to, large center angles (i.e. >60°) with small angular distributions (i.e. <5°), large center angles (i.e. >60°) with large angular distributions (i.e. >10°), small center angles (i.e. <40°) with large angular distributions (i.e. >10°), and small center angles (<40°) with small angular distributions (<5°).

Turning to FIG. **17**, a block diagram of another embodiment consistent with the present disclosure is illustrated where the vertical spacings (**Z1,Z2**) between an insulating modifier and the plane **151** defined by the front surface of the workpiece **138** may be adjusted. The insulating modifier may be the insulators **252** and **254** as detailed in other embodiments. An actuators **703a,b** may be mechanically coupled to the insulators **252** and **254**, respectively to drive the insulators in a vertical direction as shown by arrows **730**, **732** relative to the plane **151**. The **Z** positions of the insulators **252** and **254** relative to the plane **151**, and also relative to each other, influence the shape of the boundary between the plasma and the plasma sheath and also the trajectories of the ions striking the workpiece **138**. The actuators **703a,b** may be controlled by controllers, such as controllers **356a,b**. In other embodiments, a single controller is used to control both actuators **703a,b**.

FIGS. **18** and **19** are cross sectional views consistent with FIG. **17** to illustrate ion trajectories at differing **Z** positions of

the insulators **252** and **254** relative to the plane **151** with all other parameters being equal. In FIG. **18**, the insulators **252**, **254** are vertically spaced by a distance of ($Z2a-Z1$). In FIG. **19**, the insulators **252**, **254** are positioned using a second vertical spacing ($Z2b-Z1$), where $Z2b>Z2a$. Therefore, the gap angle (ψ) is greater in FIG. **19**. In FIG. **18**, the boundary **863** between the plasma and the plasma sheath has a roughly convex shape relative to the plane **151**. In contrast, in FIG. **19**, the boundary **963** has a shallower shape. The shape of the boundaries **863**, **963** combined with the Z gap distances ($Z1$) and ($Z2a, Z2b$), the gap angle (ψ), and the electric field lines in the plasma sheath, influences the center angle of the ions striking the workpiece **138**. For example, the center angle of ions striking the workpiece **138** with the relatively short vertical spacing (smaller gap angle) is closer to zero degrees (i.e. closer to striking the workpiece at a perpendicular angle) than the center angle of ions striking the workpiece **138** with the relatively greater vertical spacing (larger gap angle) shown in FIG. **19**.

In another embodiment, the vertical spacing between the insulators ($Z2-Z1$) is maintained, while $Z1$ is varied. This has the effect of moving the insulators closer (or further) from the workpiece, while maintaining the gap angle (ψ). In this embodiment, the center angle remains constant, while the angular distribution varies as $Z1$ varies. In some embodiments, the angular distribution increases as $Z1$ is decreased, while the distribution decreases as $Z1$ is increased. In other words, for example, one value of $Z1$ may result in an angular distribution of 5-10° about the center angle, while a smaller value of $Z1$ may result in an angular distribution of 20-30°. This effect may be due to the change in the shape of the boundary between the plasma and the plasma sheath, which varies as the insulators are moved relative to the workpiece.

Turning to FIG. **20**, a block diagram of another embodiment consistent with the present disclosure is illustrated where the horizontal spacing (G) between insulators **252** and **254** may be adjusted. The horizontal spacing adjustments may be in lieu of, or in addition to, the earlier detailed vertical spacing adjustments of FIGS. **18** and **19**. An actuator **912** may be mechanically coupled to at least one of the insulators **252** and **254** to drive the insulators in the direction shown by the arrow **916** relative to one another. The actuator **912** may be controlled by a controller such as controller **356**. Modification of the horizontal spacing (G) affects both the gap width (δ) and the gap angle (ψ).

In one embodiment, the horizontal gap spacing (G) between the insulators is varied. Modification of the horizontal gap spacing can be used to affect both the center angle and the angular distribution. For example, if the horizontal gap spacing is reduced to 0 or made negative by having the insulators overlap, as shown in FIG. **21**, the center angle can be made very large. Small positive horizontal gap spacings will result in large gap angles (ψ), depending on the values of $Z2$ and $Z1$, resulting in larger center angles. Large positive horizontal gap spacings will reduce the gap angle (ψ), resulting in a smaller center angle.

A bimodal angular spread **1200**, such as that shown in FIG. **23**, can be created using the configuration shown in FIG. **22**. A bimodal angular spread refers to a first center angle having a first angular distribution and a second center angle having a second angular distribution. Such a bimodal angular spread may also be created by changing the relative vertical position of only two insulators such as illustrated in FIG. **15**. In the embodiment of FIG. **22**, at least three insulators **1400**, **1402**, **1404** are used. By arranging the outer two insulators **1400**, **1404** on the same vertical plane ($Z2$), and maintaining the same horizontal spacing $G8$, $G9$ between the insulators, it is

possible to create a symmetric bimodal angular spread **1200**, centered about \pm/θ° . As described above, the center angles can be modified by varying the vertical spacing between the outer insulators **1400**, **1404** and the middle insulator **1402**, so as to vary the gap angles (ψ). The angular spread can be modified by varying the horizontal spacing ($G8$, $G9$) between the insulators **1400**, **1402**, **1404**, so as to vary the gap width (δ). An asymmetric distribution can be created by making $Z2a$ different than $Z2b$, by choosing $G8$ different than $G9$, or a combination of both actions.

While the previous embodiments show the insulators as being planar, this is not a requirement of the disclosure. FIG. **24a-c** shows several other embodiments of the insulators. FIG. **24a** shows an inverted “V” shaped insulator configuration. As described above, the plasma sheath follows the shape of the insulator. Therefore, the sheath forms a corresponding inverted “V” shape. Gaps in the insulator **1500** allow ions to pass through the insulator. The slope of the inverted “V”, as defined by ϕ , defines the center angle of the ion distribution. The gap angle (ψ) in this embodiment would be the complement of ϕ . The gaps Gc , Gd define the angular spread $\alpha1$, $\alpha2$, respectively. As can be seen when FIG. **24a** and FIG. **24b** are compared, a larger gap width (such as Gc) allows a greater angular spread than the narrower gap width Gd (i.e. $\alpha1>\alpha2$). FIG. **24c** illustrates another embodiment, in which the insulator **1502** is non-linear, curved or curvilinear, such that the gap width Ge is at an angle to the workpiece **138**. As explained above, the gap angles determine the center angle, while the widths of the gaps determine the angular spread.

Other embodiments are also possible and within the scope of the disclosure. For example, in some embodiments, two or more insulators are used, where they are spaced apart so as to create a gap between them. This gap between the insulators allows ions to pass through to a workpiece. In other embodiments, a single insulator is used, which has at least one opening or gap in it, through which ions may pass.

There are several considerations when developing a system. A higher gap angle (ψ) results in a greater center angle of the ion distribution. The length of the opening along plane **257** defines the width of the gap (δ). The gap width (δ) affects the angular spread of the ion distribution. It is important to note that these two variables are independent of one another. In other words, the gap angle (ψ) can be modified without changing the gap width (δ). Similarly, the gap width (δ) can be changed without affecting the gap angle (ψ). Another variable of interest is the distance from the gap (or either insulator) to the workpiece **138**. Again, this variable can be changed independent of the other two variables. Use of independent horizontal and vertical actuators (see FIGS. **17** and **20**) allow maximum flexibility in determining these parameters.

FIG. **25** is a block diagram of a plasma processing apparatus **1600** having a scanning system **1602** to drive an insulating modifier **248** relative to the workpiece **138**. In the embodiment of FIG. **25**, the insulating modifier **248** includes square insulating sheets **1612** and **1614** that are best seen in FIG. **26**. The scanning system **1602** may include one or more actuators **1604** mechanically coupled to the insulating sheets **1612** and **1614** to drive the same in both the vertical and horizontal directions. The actuator **1604** may be controlled by a controller such as controller **356**.

FIG. **26** is plan view of the square insulating sheets **1612** and **1614** and a disk shaped workpiece **138** to illustrate one example of relative movement between the same. In the embodiment of FIG. **26**, the scanning system **1602** may drive the square insulating sheets **1612** and **1614** from Position A, to Position B, and Position C, etc. so that all portions of the workpiece **138** are exposed to the gap defined by the square

insulating sheets **1612** and **1614**. If a Cartesian coordinate system is defined as detailed in FIG. **26**, the insulating sheets **1612** and **1614** are driven in the X direction of FIG. **26**. In other embodiments, the insulating sheets **1612** and **1614** or another set of different insulating sheets may be driven in the Y direction or any angle between the X and Y directions. In addition, the workpiece **138** may be rotated as the scanning system **1602** drives the insulating sheets **1612** and **1614** in one direction. The workpiece **138** may also be rotated by a pre-determined rotation angle after the scanning system **1602** drives the insulating sheets in one direction. In one example, the rotation may be about a central axis of the workpiece as illustrated by arrow **1624**.

Although the scanning system of FIG. **25** is shown with two insulating plates at a vertical spacing from one another, other embodiments are possible. For example, the scanning system can be made using three insulating plates, thereby creating two gaps, as shown in FIG. **22**. Additionally, the alternate shapes, such as those shown in FIG. **24** can be used in the scanning system. Furthermore, the patterns shown in these figures can be replicated, such that there are multiple gaps across the width or length of the workpiece. In some embodiments, all gaps produce the same angular distribution (as shown in FIG. **15-16**). In other embodiments, the gaps produce opposite distributions at $\pm\theta$ (as shown in FIG. **22-23**). In other embodiments, the gaps are used to produce varied angular distributions. In this embodiment, the final angular distribution experienced by the workpiece would be the sum of the various angular distributions.

Turning to FIG. **27**, a scanning system **1602** consistent with FIG. **25** is illustrated. Compared to FIG. **25**, the scanning system **1602** of FIG. **27** includes a plurality of insulators **1702-1**, **1702-2**, **1702-3**, . . . **1702-(n-1)**, and **1702-n** that define a plurality of gaps there between **1703-1**, **1703-2**, . . . **1703-n**. The scanning system may drive the plurality of insulators **1702-1**, **1702-2**, **1702-3**, . . . **1702-(n-1)**, and **1702-n** relative to the workpiece **138** so the plurality of gaps **1703-1**, **1703-2**, . . . **1703-n** pass over the workpiece **138**.

Modification of the gap angle (ψ) can be done by varying the gap spacing, or by varying the vertical spacing (**Z2-Z1**). Changes to gap angle may affect the center angle. Modification of the angular distribution can be done by varying the height of the insulators (**Z1**) or by changing the gap spacing. Modifications to all three parameters (**Z2**, **Z1** and gap spacing) can be employed to create a desired center angle with a desired angular distribution or spread.

In addition, it may be beneficial or advantageous to cool the insulators **252** and **254**. In some embodiments, these insulators may have channels embedded in them, whereby fluid, such as liquid or gas, may pass through, to remove heat. In other embodiments, the insulators may be good thermal conductors and may be in contact with a thermal sink.

As mentioned above, the sheath modification can be used to perform a variety of plasma processing steps. For example, a deposition or etch process can utilize these techniques. For instance, with respect to deposition, it is often necessary in semiconductor processing to deposit a conformal (i.e. equal thickness) film in a high aspect ratio gap.

In this processing, material from the plasma is deposited on the surface of the workpiece, thereby creating a film atop the workpiece. This can be done a plurality of times to create varying film thicknesses. Three dimensional features are more difficult to deposit upon, as the surfaces of the feature may be vertical with respect to the top surface of the workpiece. Greater aspect ratios are even more difficult to deposit upon. An aspect ratio is defined as the depth (or height) of a particular feature, such as a spacer or trench, divided by its

width. As device geometries shrink, void-free filling of high aspect ratio spaces (where high aspect ratio is defined to be greater than 3.0:1) becomes increasingly difficult due to limitations in existing deposition processes.

The formation of liners in trenches and spacers are examples of such difficult processes. A major challenge for integrating low dielectric constant films into copper damascene stacks is sealing the interface between the porous dielectric film and the conducting copper diffusion barrier at the trenches, especially the sidewalls.

Plasma Enhanced Chemical Vapor Deposition (PECVD) is one possible process that can be used to form these liners. However, the performance of line-of-sight processes is limited by the aspect ratio of the three dimensional feature. As aspect ratios increase, coverage and therefore performance of the sealing process decreases.

Lining trenches is but one example of a plasma process that requires modification to traditional PECVD processes. Deposition of doped (i.e. boron or phosphorus doped) silicon films to form three-dimensional devices is another example. Formation of air gaps at the interconnect levels is yet another example.

FIGS. **28b-c** show a variety of three dimensional features, which can be conformally deposited using the PECVD process described in this disclosure. FIG. **28a** shows a conventional flat workpiece surface. Such a surface is best deposited with ions or neutrals, all of which are perpendicular or nearly perpendicular to the surface of the workpiece. FIG. **29a** shows the ion angular distribution of the optimal deposition. Such a deposition is done without any modification of the plasma sheath.

FIG. **28b** shows a narrow, deep trench compared to the trench of FIG. **28c**. This trench has a left sidewall **1720**, a right sidewall **1722** and a bottom surface **1724**. A uniform coating or layer **1726** is applied to the surface of the substrate, including the substrate surface **1728**, the sidewalls **1720**, **1722** and the bottom surface **1724**. Clearly, an incident beam which is only perpendicular to the substrate surface **1728** can only be used to coat the substrate surface **1728** and the bottom surface **1724**. The angle of incidence is defined with respect to a line perpendicular to the workpiece plane **151**. Thus, an angle of incidence of 0° is perpendicular to the workpiece plane **151**. Trajectory **1730** has an angle of incidence of 0° , while trajectory **1732** has a greater angle of incidence than trajectory **1734**. Trajectory **1734** is shown having an angle of incidence of θ_1 .

To properly and uniformly deposit material on the sidewalls, it is necessary to have a modified ion angular distribution. The ions having an angle of incidence of 0° (trajectory **1730**) deposit material on the substrate surface **1726** and bottom surface **1728**. Ions having an angle of greater than a particular value (such as those traveling along trajectory **1732**) can deposit material only on the upper of the sidewalls **1720**, **1724**, as the top surface **1728** casts a shadow which stops ions from reaching the lower portions of the sidewalls. Ions with an angle of incidence **1734** less than this particular value are able to deposit material on all portions of the sidewalls **1720**, **1722**. Thus, if the depth of the feature is represented by the variable, d , and the width of the feature is represented by the variable w , the maximum angle of incidence, θ_1 , capable of depositing material on the bottom portion of the sidewall is defined by:

$$\tan \theta_1 = w/d, \text{ or } \theta_1 = \arctan(w/d)$$

Angles greater than θ_1 can only deposit material on a portion of the sidewall, thereby creating an uneven layer of material.

FIG. 30a shows the feature of FIG. 28b. Various points (Q-Z) are labeled on the workpiece and within the feature. For example, Q,R,S are on the workpiece to the left of the feature, while points X,Y,Z are on the workpiece to the right of the feature. Points T,W are along the sidewalls of the feature, and points U,V are on the bottom surface of the feature.

FIGS. 30b-f show various timing diagrams. It is assumed that the gap described above is scanned relative to the workpiece, such that the gap is moving from the left to the right of the feature (as shown in FIG. 30a). Each timing diagram shows the height that is being deposited as a function of time.

For example, FIG. 30b shows the timing diagram when an angle of incidence of 0° is used. In this embodiment, the material is deposited along the surface of the workpiece as the gap moves to the right. Once the opening is directly above the feature (i.e. point S), the depth of the deposition changes, corresponding to the bottom of the feature. When the gap is directly above point X, the height changes again, as the deposition now occurs on the surface of the workpiece. Notice that the sidewalls cannot be deposited using an angle of incidence of 0° .

FIG. 30c shows a timing diagram for an angle of incidence less than θ_1 (defined as $\arctan(w/d)$). In this figure, the ions reach a portion of the workpiece to the left of the gap. In other words, when the gap is directly over point S, the ions are targeted toward a point between R and S. Therefore, the first portion of FIG. 30c is a delayed version of FIG. 30b. When the gap reaches a point where the ions contact point S, further lateral movement of the gap will cause the ions to strike the left sidewall, reaching points T and U. Since the angle of incidence is less than θ_1 , the entire sidewall is deposited. As the gap continues to move to the right, eventually the ions cannot deposit the feature, as the workpiece surface (i.e. point X) blocks the ions. At this point, the ions continue to deposit on the top surface of the workpiece, again as a delayed version of FIG. 30b. Since the ions are angled to the left, the right sidewall is never deposited.

FIG. 30d shows a timing diagram for an angle of incidence greater than θ_1 . This diagram closely resembles FIG. 30c with several important differences. First, the diagram is further delayed with respect to the top surface (i.e. Q,R,S,X,Y,Z). Also, due to the increased angle of incidence, the ions cannot reach the bottom of the feature (point U) before being blocked by the top surface (point X). As a result, the bottom surface and the right sidewall are not deposited.

FIG. 30e shows a timing diagram for an angle of incidence that is negative, but greater than $-\theta_1$. This figure corresponds to FIG. 30c, in that the ions reach the entire sidewall and also a portion of the bottom of the feature. Since the ions are directly downward and to the right, the right sidewall is deposited, but the left sidewall is not.

FIG. 30f shows the timing diagram for an angle of incidence that is more negative than $-\theta_1$. This figure shows that the ions never reach the bottom surface of the feature, and only are deposited on a portion of the right sidewall.

By choosing the correct range for the angle of incidence, it is possible to create the desired deposition of a three dimensional feature. The diagrams of FIG. 30b-f are examples and the locations of the points Q-Z are only intended to illustrate the effects of changing the angle of incidence.

FIG. 28c shows a wide, shallow trench compared to FIG. 28b. This trench has a left sidewall 1740, a right sidewall 1742 and a bottom surface 1744. A uniform coating or layer 1746 is applied to the surface of the substrate, including the substrate surface 1748, the sidewalls 1740, 1742 and the bottom surface 1744. As below, to properly and uniformly deposit material on the sidewalls, it is necessary to have a modified

ion angular distribution. The ions having an incident angle of 0° (those traveling along trajectory 1750) deposit material on the substrate and bottom surfaces. Ions having an incident angle greater than about 70° , such as those ions following trajectory 1752 can deposit material only on the upper portions of the sidewalls 1740, 1742, as the top surface 1728 casts a shadow which stops ions from reaching the lower portions of the sidewalls. Ions with a relatively smaller angle of incidence, e.g., those following trajectory 1754 are able to deposit material on all portions of the sidewalls 1740, 1742 and on the bottom surface 1744. Thus, if the depth of the feature is represented by the variable, d, and the width of the feature is represented by the variable w, the maximum incident angle θ_2 , capable of depositing material on the bottom portion of the sidewall is defined by:

$$\tan \theta_2 = w/d, \text{ or } \theta_2 = \arctan(w/d)$$

In this case, the width (w) is much greater than the depth (d), therefore $\theta_2 > \theta_1$ (FIG. 28b). In one embodiment, θ_1 may be 30° , while θ_2 may be 50° . Thus, a wider ion angular distribution may be used.

In all cases, the maximum desired ion angular distribution is related to the aspect ratio of the three dimensional feature to be deposited. Narrow, deep features require a smaller range of angular distribution as shown in FIG. 29b, while wide, shallow features can utilize a broader range of angular distribution, as shown in FIG. 29c.

Thus, the disclosed embodiments can be utilized to produce conformal deposition of three dimensional features. The plasma sheath is manipulated to create an ion angular distribution in accordance with FIG. 29b, where θ is defined based on the aspect ratio of the three dimensional feature to be deposited upon. As described with respect to FIGS. 4-5, the angle of incidence of incoming ions can be manipulated to create an angular distribution, centered around 0° , of $\pm\theta$. In some embodiments, θ is based on arctangent (w/d) where w is the feature width and d is defined as the feature depth. This is done by varying the size of the gap, and its vertical spacing from the workpiece, as shown in FIGS. 7-10.

In some embodiments, it may be desirable to deposit material in a three dimensional feature, while leaving an air gap beneath the deposition. FIG. 31a shows a three-dimensional feature 1900, having sidewalls 1902, 1904 and a bottom surface 1905. Material 1906 is deposited in such a way so as to leave an air gap 1908 between the deposited material 1906 and the bottom surface 1905.

Such a configuration can be created by properly modifying the ion angular distribution. For example, based on the description above, it is clear that the incoming ions cannot have an incident angle perpendicular to the workpiece, as this would deposit material on all horizontal surfaces, including bottom surface 1905. Furthermore, ions having a low angle of incidence are capable of reaching the bottom surface 1905 and the lower portions of the sidewalls 1902, 1904. Thus, to achieve the desired pattern, a different angular distribution is required, as shown in FIG. 31b. The angle distribution is bimodal, centered about -0° and 0° . As before, the preferred angular distribution is related to the aspect ratio of the feature 1900. In this case, assume that the depth of the feature is d and its width is w. Further assume that the height of the desired air gap 1908 is given by h. The angle of incidence cannot be less than that defined by:

$$\tan(\theta_3) = w/(d-h), \text{ or } \theta_3 = \arctan(w/(d-h)).$$

FIG. 31*b* shows a bimodal angular distribution which would achieve the pattern shown in FIG. 31*a*. Insulators disposed in the configuration shown in FIG. 22 can be used to create this bimodal angular distribution.

As described above, the plasma sheath can be manipulated to vary its shape. While the above disclosure suggests use of a time invariant angular distribution, based on a specific sheath shape, the disclosure is not limited in this way. For example, as material is deposited on the two sidewalls, the width of the feature decreases at a higher rate than the depth. Therefore, the aspect ratio of the feature increases. Thus, to counteract this effect, the sheath can be manipulated over time to decrease the angular distribution, based on the increased aspect ratio.

Thus, to conformally deposit a three dimensional feature, one may use an ion angular distribution based on the initial aspect ratio, as described above. As material is deposited on the sidewalls and bottom surface, the aspect ratio necessarily increases. This requires a corresponding decrease in the angular distribution. This process is repeated until the desired amount of material has been deposited on the sidewalls and the bottom surface. As described above, the angular distribution is adjusted by varying the separation of the insulators 212, 214 (see FIG. 8) or the distance between the insulators 212, 214 and the workpiece 138 (see FIG. 10). This adjustment can be made continuously, based on the deposition rate, or can be made in discrete steps as required. In some embodiments, plasma parameters can be modified during the process. In other embodiments, the implant energy can be modified during the process.

In another example, consider the feature shown in FIG. 31*a*. As described above, a bimodal ion angular distribution is used to create a layer of material spaced above the bottom surface. The center angles of the bimodal distribution are related to the aspect ratio of the feature and the desired height of the air gap. Once that layer is formed, the angular distribution can be modified. For example, the two bimodal center angles can be decreased, to deposit more material on top of the previous deposited material. This process can continue until the center angles reach 0°. This allows the feature to be filled as shown in FIG. 31*a*. In another embodiment, after the layer of material has been deposited and the air gap 908 is formed, a traditional angle of incidence of 0° can be used to layer more material onto the previously deposited layers.

Furthermore, this method of using varying angles of incidence need not be used only for conformal deposition. This process can be modified so as to create an uneven ion flux if desired. In addition, the use of a deposition based on a modified sheath shape can be combined with other steps. For example, a traditional (orthogonal) deposition may precede or follow the conformal deposition process described above. For example, the ion angular distribution shown in FIG. 31*b* can be used to create the air gap 1908 in the trench. A traditional orthogonal deposition may then be subsequently employed to increase the thickness of the coating. Alternatively, the traditional PECVD may be applied first, followed by a directional deposition.

This deposition method can be applied to a variety of films and deposition precursors. For example, materials such as but not limited to organosilicon precursors (methysilanes, hexamethyldisiloxane (HMDSO), octamethyltetrasiloxane (OMCTS), and tetramethyltetrasiloxane (TMCTS)) can be used for deposition of SiCOH for pore sealing applications and formation of air gaps. SiH₄ can be used for deposition of SiO₂ and SiN lines and spacers. Organometallic precursors can be employed for deposition of liners and diffusion barriers

in vias and lines. Finally, SiH₄/B₂H₆/PH₃/AsH₃ mixtures can be used for three dimensional deposition.

In addition to deposition, manipulation of the plasma sheath can be employed for etching processes as well. During plasma etching, ions and neutrals are created and controlled to affect the sidewall profile of the three-dimensional feature being etched. In some embodiments, a straight (i.e. vertical) sidewall is desired. This is performed using an anisotropic etch, wherein the ions are directed orthogonally to the surface of the workpiece. Examples where this type of etching is used include gate stack, BEOL damascene and FinFET. FIG. 32*a* shows a feature 2002 which is etched by orthogonally directed ions 2010. The portions of the substrate 2004 which are not to be etched are protected by a mask 2000. As all ions are orthogonal to the surface of the substrate 2004, the etched region 2002 has vertical sidewalls. FIG. 29*a* shows the ion angular distribution necessary to create this feature.

In other embodiments, an isotropic etch is desirable, and is typically done using wet chemistry (e.g. S/D etch prior to epi deposition for improved overlap). In certain embodiments, it is desirable to have trenches or other three-dimensional features where the sidewalls are not vertical, but rather are tapered. FIG. 32*b* shows such a feature where the sidewalls are slightly tapered. Note that the increased ion distribution allows the sidewalls to be etched beneath the mask in the horizontal direction.

In one embodiment, ions having a wide angular spread (such as greater than 40°, as shown in FIG. 29*c*) are impacted on the workpiece 2024. This etches the workpiece 2024 in all areas not protected by a mask 2020. Since a wide angular spread is used, the ions 2030 having the greatest angle of incidence are able to etch material 2026 that is positioned below the mask 2020. A small wedge 2028 of substrate remains beneath the mask, as it is protected by mask 2020. By increasing the ion angular spread (i.e. allowing a greater maximum angle of incidence), the amount of material 2026 under the mask that is etched can be increased, thereby increasing the degree of taper. As the material is etched away, the angular distribution is reduced, so that the maximum angles of incidence are reduced. An example angular spread is shown in FIG. 29*b*. The decrease in angular spread tends to focus the etching on a narrower area. As the process continues, the angular spread can continuously reduced, until it becomes the traditional spread, such in FIG. 29*a*. The rate at which the angular spread is varied with time determines the sidewall shape. The taper 2031 is based partly on the initial angular spread and the rate at which the angular spread is decreased. A slow decrease in angular spread yields a feature having a slight taper 2031. A more rapid decrease in angular spread increases the taper of the feature.

As explained, the tapered effect shown in FIG. 32*b* can be created using this method. Additional shapes, such as those shown in FIGS. 32*c* and 32*d*, can also be created by using an angular distribution, centered around 0°, and varying the angular spread as a function of time. To create the shape shown in FIG. 32*b*, the process begins by using a wide angle. This angle etches material near the top of the sidewalls. As the trench deepens, the angular spread is reduced, which causes the resulting sidewalls to become tapered. FIG. 32*c* uses a similar profile as used to create the feature of FIG. 32*b*, however the duration of the ion beam having an angle of incidence of 0° (see FIG. 29*a*) is reduced, as compared to the duration of this ion beam when used to create the profile shown in FIG. 32*b*. Furthermore, the starting angular distribution is greater than that used to create the shape shown in FIG. 32*b*. The feature of FIG. 32*d* is created using a wide

angular spread, such as greater than 40°, as shown in FIG. 29c, with little or no reduction in angular spread over time.

FIG. 33a show a three dimensional feature 2100 in which the taper of the sidewalls 2102 is greater than 90 degrees. 90 degrees is defined as vertical to the surface of the workpiece. Tapers greater than 90 degrees imply that the feature increases in width as the depth increases. To etch the feature 2100 in this manner, an ion angular distribution, as shown in FIG. 31b may be used. The bimodal nature of the incident ions creates two etched regions 2104, 2106, each of which is roughly parallel to one of the center angles of incidence. In FIG. 33a, the angle of incidence is sufficiently large such that a portion 2110 of the bottom surface of the feature 2100 is not completely etched. The size of this remaining portion 2110 is a function of the incidence angle, the width of the opening in the mask 2112, and the depth of the feature 2100.

For example, the innermost edges of the etched region are defined as the first portion of the substrate which has a line-of-sight to the ion beam. These positions are designated as $\phi 1$ and $\phi 2$. $\phi 1$ is offset from the right corner of the mask by a distance equal to $d \cdot \tan(\Theta)$, where d is the depth of the feature 2100 and Θ is the angle of incidence. If the opening in the mask 2112 is given by w , then an unetched portion 2110 will exist if $d \cdot \tan(\Theta)$ is greater than $w/2$.

To eliminate this unetched portion 2110, a second angular distribution, centered at 0° or a traditional orthogonal distribution (see FIG. 29a), can be employed after the bimodal ion angle distribution is complete. Such a feature can be seen in FIG. 33b.

It could also be achieved by performing an over-etch step where a etch barrier is used between two layers. In the etching process, there are different selectivities between materials, such that some material will not etch with the plasma used. Thus, the etching process will then stop at this layer.

Other feature shapes can be generated by combining the bimodal ion distribution, shown in FIG. 31b, with an angular distribution, entered around 0° (such as those shown in FIGS. 29a, 29b and 29c). FIGS. 33c and 33d show two feature shapes that can be created by modifying the angular distribution with time, so that it may utilize both a 0° centered angular distribution and a bimodal angular distribution. For example, the shape in FIG. 33c can be created by starting with an etch having no angular spread (see FIG. 29a). This creates a vertical trench, as is known in the art. Later, a wide angular spread is used, which etches material so as to form the desired shape. The shape shown in FIG. 33d can be created using isotropic etching.

The terms “angle of incidence” and “incident angle” are used interchangeable throughout this disclosure, and have the same meaning. Specifically, the angle of incidence is the angle at which ions strike the workpiece. It is measured as a deviation from a line that is perpendicular to the plane 151 defined by the front surface of the workpiece. In other words, ions that strike the workpiece perpendicularly have an angle of incidence or incident angle of 0°.

Accordingly, there is provided methods of performing plasma processing on a feature on a workpiece. In certain embodiments, the shape of the plasma sheath is modified and then material from the plasma is deposited on the feature. In a further embodiment, the modification of the plasma sheath varies in relation to the aspect ratio of the feature. In still other embodiments, the modification of the plasma sheath also varies over time, as material is deposited on the feature. Modification of the plasma sheath can also be used to perform etching of a workpiece. Various modifications of the plasma sheath can be performed to vary the shape and profile of the etched feature.

The present disclosure is not to be limited in scope by the specific embodiments described herein. Indeed, other various embodiments of and modifications to the present disclosure, in addition to those described herein, will be apparent to those of ordinary skill in the art from the foregoing description and accompanying drawings. Thus, such other embodiments and modifications are intended to fall within the scope of the present disclosure. Further, although the present disclosure has been described herein in the context of a particular implementation in a particular environment for a particular purpose, those of ordinary skill in the art will recognize that its usefulness is not limited thereto and that the present disclosure may be beneficially implemented in any number of environments for any number of purposes. Accordingly, the claims set forth below should be construed in view of the full breadth and spirit of the present disclosure as described herein.

What is claimed is:

1. A method of etching a three dimensional feature, having a desired width, depth and taper, in a workpiece, comprising:
 - generating a plasma having a plasma sheath adjacent to a front surface of the workpiece; and
 - modifying a shape of a boundary between the plasma and the plasma sheath while accelerating material from the plasma across the boundary to etch the three dimensional feature on the front surface of the workpiece wherein the material strikes the three dimensional feature at a range of incident angles, and wherein the range of incident angles is dependent on the shape of the boundary between the plasma and the plasma sheath.
2. The method of claim 1, wherein the range of incident angles includes a center angle and a distribution about the center angle.
3. The method of claim 2, wherein the three dimensional feature is inwardly tapered, such that its desired width at the front surface of the workpiece is greater than its desired width at a bottom of the three dimensional feature, and the center angle is perpendicular to a plane defined by the front surface of the workpiece and the distribution is greater than zero degrees.
4. The method of claim 2, wherein the three dimensional feature is outwardly tapered, such that its desired width at the front surface of the workpiece is less than its desired width at a bottom of the three dimensional feature, and the range of incident angles comprises two center angles, each having a distribution.
5. The method of claim 2, wherein the modification of the boundary comprises:
 - selecting a first center angle and a first distribution based on the desired taper; and
 - directing material toward the three dimensional feature using the first center angle and the first distribution, whereby the material etches the workpiece to a first depth.
6. The method of claim 5, further comprising:
 - selecting a second center angle and a second distribution based on the desired taper and the first depth; and
 - directing material toward the three dimensional feature using the second center angle and distribution, whereby the material etches the workpiece to a second depth.
7. The method of claim 6, further comprising repeating the selecting and directing steps a plurality of times until a desired depth has been etched.
8. The method of claim 7, wherein the distribution is reduced over time.
9. The method of claim 7, wherein the incident angle is reduced over time.